

New Advances in Topology Optimization

Session Organizers: Gláucio H. PAULINO (UIUC), Emílio SILVA (University of São Paulo)

Keynote Lecture

Topology optimization with adaptive mesh refinement

Eric DE STURLER* (Virginia Tech), Gláucio H. PAULINO, Shun WANG (University of Illinois at Urbana-Champaign)

Strategies for computational efficiency in continuum structural topology optimization of sparse 3D systems

Colby C. SWAN*, Salam F. RAHMATALLA (University of Iowa)

Wachpress elements for topology optimization

Cameron TALISCHI*, Gláucio H. PAULINO, Chau H. LE (University of Illinois at Urbana-Champaign)

Topology optimization technique considering both static and dynamic characteristics of the structures

S. J. LEE*, J. E. BAE (Gyeongsang National University)

Keynote Lecture

Topology optimization method utilizing iterative solvers with subspace recycling applied to high-resolution electrical impedance tomography

Luís Augusto Motta MELLO*, Emílio Carlos Nelli SILVA (University of São Paulo), Eric DE STURLER (Virginia Tech), Gláucio H. PAULINO (University of Illinois at Urbana-Champaign)

Topology optimization considering fabrication errors and length scale constraints

James K. GUEST (Johns Hopkins University)

A simple and effective inverse projection scheme for void distribution control in topology optimization

Gláucio H. PAULINO* (University of Illinois at Urbana-Champaign), Sylvia ALMEIDA (Universidade Federal de Goiás), Emílio Carlos Nelli SILVA (University of São Paulo)

Design of dynamic laminate piezoelectric sensors and actuators using topology optimization

Paulo Henrique NAKASONE*, Emílio Carlos Nelli SILVA (University of São Paulo)

For multiple-author papers:

Contact author designated by *

Presenting author designated by underscore

Topology optimization with adaptive mesh refinement

Eric DE STURLER*, Glaucio H. PAULINO, Shun WANG

*Department of Mathematics, Virginia Tech
544 McBryde Hall, Virginia Tech, Blacksburg, Virginia 24061-0123
sturler@vt.edu

Abstract

We outline a robust method for topology optimization with adaptive mesh refinement and derefinement (AMR). Since the total volume fraction in topology optimization is usually modest, after a few initial iterations the domain of computation is largely void. It is inefficient to have many small elements in such regions, as these contribute significantly to the overall computational cost but little to the accuracy of computation and design. At the same time, we want high spatial resolution for accurate three-dimensional designs to avoid significant postprocessing or interpretation. AMR offers the possibility to balance these two requirements, but it has received little attention in the context of topology optimization. We will discuss approaches by Costas and Alves [2] and Stainko [3]. Unfortunately, both approaches may lead to suboptimal designs that are mesh dependent. We extend these approaches to obtain a method that yields optimal designs, and we show experimentally that our improvements lead to designs that are equivalent to designs computed on uniform meshes at the finest level of refinement. Furthermore, we demonstrate significant reductions of run time by using AMR and efficient methods for the solution of the resulting large, linear systems, following Wang et al. [4].

1. Introduction

Topology optimization is a powerful structural optimization method that combines a numerical solution method, usually the finite element method, with an optimization algorithm to find the optimal material distribution inside a given domain. In designing the topology of a structure we determine which points in the domain should be material and which points should be void; see Bendsoe and Sigmund [1].

In topology optimization, problems are solved most commonly on fixed uniform meshes with a relatively large number of elements in order to achieve accurate designs. However, as void and solid regions appear in the design, it is more efficient to represent the holes with fewer large elements and the solid regions, especially the material surface, with more fine elements. Since the shape and position of holes and solid regions are initially unknown, the most economical mesh representation for the design is unknown a priori. Therefore, adaptive mesh refinement (AMR) is very suitable for topology optimization. *The purpose of AMR for topology optimization is to get the design that would be obtained on a uniformly fine mesh, but at a much lower computational cost by reducing the total number of elements and having fine elements only where and when necessary.*

Highly accurate designs on uniform meshes may require so many elements that the solution of the optimization problem becomes intractable. However, AMR leads to high resolution in the mesh only when and where necessary. This makes it possible to do highly accurate designs with a modest number of elements against a reasonable cost. Obviously, we do not want the use of AMR or the AMR procedure to alter the computed designs. However, there is a risk of this, since the mesh influences the computed deformations and sensitivities. So, the solutions from the finite element analysis using AMR must be as accurate as those obtained on a uniform fine mesh. Moreover, it must be the accurate solution and corresponding sensitivities obtained on the finest mesh that govern the design. If coarse mesh solutions drive or limit the design, suboptimal designs may result when designs optimal on a coarser mesh differ substantially from the optimal design on a (much) finer mesh; see Wang et al. [5]. The early work in this area, though leading to acceptable designs in specific instances, does

not satisfy these properties. We propose simple but essential changes to these methodologies that lead to AMR based designs that are equivalent (up to some small tolerance) to designs on uniform fine meshes.

2. Topology Optimization in a nutshell

In topology optimization we solve for the material distribution in a given design domain Ω . Here, we minimize the compliance of a structure under given loads as a function of the material distribution. To solve this problem numerically, we discretize the computational domain using finite elements, where we use a lower order interpolation for the density field (material distribution) than for the displacement field. We take the most common approach using trilinear interpolation for the displacement field and constant density in each element. The compliance minimization problem after finite element discretization is defined as

$$\begin{aligned} \min_{\forall e \rho_e \in [\rho_0, 1]} \mathbf{f}^T \mathbf{u} \\ \text{s.t.} \quad \begin{cases} \mathbf{K}(\boldsymbol{\rho}) \mathbf{u} = \mathbf{f} & \text{for } x \in \Omega \setminus \Omega_0, \\ \mathbf{u} = \mathbf{u}_0 & \text{for } x \in \Omega_0, \\ \sum_e \rho_e V_e \leq V_0, \end{cases} \end{aligned}$$

with ρ_e the density in element e , $\boldsymbol{\rho}$ the vector of element densities, \mathbf{K} the stiffness matrix, which is a function of the element densities, V_e the volume of element e , V_0 the maximum total volume (fraction) for the design, and Ω_0 the part of the domain where the displacement is prescribed. We enforce a small positive lower bound, $\rho_0 = 10^{-3}$, on the element density to avoid singularity of the stiffness matrix.

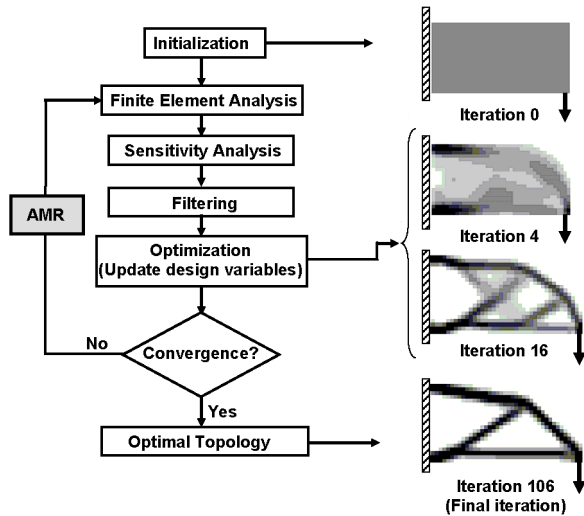


Figure 1. Overview Topology Optimization Algorithm

The Solid Isotropic Material with Penalization method (SIMP) is used to make intermediate

densities unfavorable; we define the elasticity tensor as a function of the element density, $E_e = \rho_e^p E_0$, where p is the penalization parameter. With $p > 1$, intermediate densities provide little stiffness per (unit) volume. The common choice, $p = 3$, results in intermediate material properties satisfying the Hashin-Shtrikman bound for composite materials; see Bendsøe and Sigmund [1]. We apply continuation on p to avoid problems with local minima, starting with $p = 1$ and slowly increasing p as the design converges.

The general scheme for topology optimization using AMR is illustrated in Figure 1. Various optimization algorithms can be used for topology optimization. For this paper, we use Optimality Criteria (OC); see Bendsøe and Sigmund [1]. Dynamic mesh adaptation may be carried out before the finite element analysis.

3. Dynamic, Adaptive Mesh Refinement

Little research has been done in applying AMR to topology optimization. So, we briefly discuss two recent, important, papers in this area. The AMR method by Costa and Alves [2] goes through a predetermined, fixed sequence of optimizations and subsequent mesh refinements (they do not use derefinement), using (assuming) a converged solution on a 'coarse mesh' to guide the refinement of that mesh and start the optimization on the next 'fine mesh'. Coarse meshes and the solutions on these coarse meshes are never revisited or updated after generating the next finer mesh. The method aims at refining the coarse mesh design; after a fixed number of optimization steps on a given mesh, they refine all material elements and elements on the boundary between material and void. Stainko [3] follows a slightly different approach with respect to the refinements. Mesh refinement is done only along the material boundary as indicated by the (regularization) filter. So, elements

completely inside a material region or a void region are not refined. These approaches share two important choices that may lead to problems. First, both approaches solve the design problem on a fixed mesh until convergence and then refine. After refinement on a given level, the mesh on that level remains fixed for the remainder of the optimization. Therefore, all further refinements are constrained by the converged coarser level solutions. This works well in terms of refining the design, but for many design problems the optimal solution on a uniform fine(st) mesh is quite different from the converged solution on a coarser mesh. In that case, mesh refinement based only on the coarser level solution will erroneously confine the solution on the finer mesh to a smooth version of the coarser level solution. Therefore, the approaches proposed in Costa and Alves [2] and Stainko [3] may lead to suboptimal designs; see Wang et al. [5]. Second, both approaches lack derefinement. This may lead to inefficiencies, having too many elements.

Next, we briefly describe the main ideas for our AMR strategy for topology optimization. Space restrictions prevent us from giving a detailed description, and we refer to Wang et al. [5] for details and implementation. We base our algorithmic choices on a set of requirements on AMR codes for topology optimization. As stated above, the purpose of AMR for topology optimization is to get the design that would be obtained on a uniform fine mesh, but at a much lower computational cost by reducing the total number of elements and having fine elements only where (and when) necessary.

First, since the finite element analysis and the computation of sensitivities drive the changes in material distribution, they should be as accurate as on the uniform fine mesh. Therefore, we need a fine mesh that covers at least the material region and the boundary. Since the void regions have negligible stiffness they do not influence the (intermediate) linear finite element solutions and sensitivity computations. So, we do not need a fine mesh inside the void regions. Hence, we use a refinement criterion similar to that of Costa and Alves [2]. At this point we focus on refinement and derefinement for shape only. Therefore, we are conservative with respect to accuracy, and we expect that, in future implementations, good error indicators will lead to further efficiency gains, in particular because of derefinement in solid material regions. Second, the accurate computations on the finest level should drive the changes in the material distribution. This requires continual mesh adaptation so that computational results after refinements can drive updates to the material distribution, and designs are not confined by earlier coarse grid results. This also means that as the material region moves close to the boundary between fine and coarse(r) mesh, additional refinements allow for further evolution. Third, we need to ensure that the design can change sufficiently in between mesh updates. Therefore, we maintain a layer of additional refinements around the material region (in the void region) and carry out continual mesh adaptation. Due to the additional layer of refinements and continual mesh updates, the design can change arbitrarily following the fine grid computations and resulting sensitivities, and it is not confined by earlier coarse grid results. To ensure that the design accurately reflects the fine mesh computations, we allow rapid refinements of the mesh early on when voids and material regions (and hence the boundary) develop. Fourth, since the design can change substantially from its estimate on a coarse mesh, we may have fine elements in void regions. Those elements must be removed for efficiency, so we need derefinement. A hierarchical representation of adaptive meshes facilitates our strategy of continual mesh refinement and derefinement.

4. A Numerical Experiment: Computing an Optimal Cantilever Beam

We compute the optimal design for the three-dimensional cantilever beam shown in Figure 2. Exploiting symmetry, we discretize only a quarter of the domain. We solve this problem first on a (fixed) uniform mesh with $128 \times 32 \times 32$ B8 elements and then following our AMR strategy. The initial mesh for the AMR-based design has $64 \times 16 \times 16$ B8 elements. The final results are shown in Figure 3, with the AMR solution on the left and the uniform mesh solution on the right. We measure the relative difference between two designs as follows

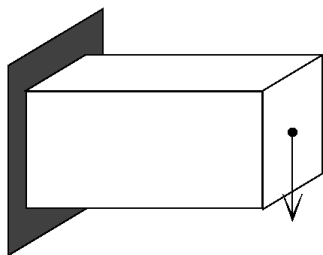


Figure 2. 3D Cantilever beam with domain scale 2:1:1

$$D(\rho^{(1)}, \rho^{(2)}) = \frac{\int_{\Omega} |\rho^{(1)} - \rho^{(2)}| d\Omega}{\int_{\Omega} \rho^{(1)} d\Omega}. \quad (1)$$

The relative difference between these two designs, as defined by (1), is only 0.0909%.

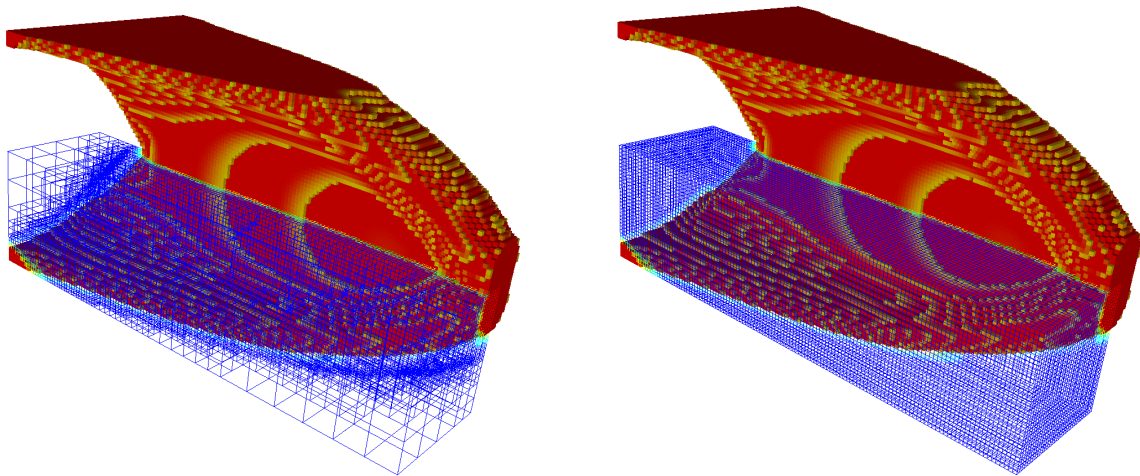


Figure 3. Final AMR solution of the optimal 3D Cantilever beam problem and final solution on a fixed uniform mesh (128 x 32 x 32). The finest elements in both meshes are the same size. The relative difference in density distribution of both designs is only about 0.1%.

We use the incomplete Cholesky-preconditioned, recycling minimum residual solver (RMINRES) proposed by Wang et al. [4] to solve the linear systems arising from the finite element discretization for a given material distribution. The dimensions of the linear systems of equations for the adaptive mesh are less than half of those for the uniform, fine mesh. The difference is even larger early in the optimization iteration. Moreover, the number of RMINRES iterations for the linear systems derived from the AMR mesh are smaller than those from the uniform, fine mesh, as the adaptive meshes lead to better conditioned linear systems. *In total, using AMR reduces the solution time roughly by a factor three.*

5. Conclusions

We have used AMR to reduce the total runtime for a three-dimensional topology optimization problem by a factor three while obtaining essentially the same design as on a fixed uniform fine mesh. Fast iterative solvers also play an important role in our approach. AMR provides a promising future research direction in topology optimization; especially important are efficiently updating preconditioners and combining refinement and derefinement for shape with refinement and derefinement based on a posteriori error estimates.

Acknowledgements

We are indebted to Hong Zhang and Mat Knepley from Argonne National Laboratory for their help with the PETSc library and to Roy Stogner, John Peterson, and Benjamin Kirk from the University of Texas at Austin for their help with the libMesh library.

References

- [1] Bendsøe MP and Sigmund O. *Topology Optimization: Theory, Methods, and Applications*. Springer-Verlag, Berlin, 2003.
- [2] Costa Jr. JCA and Alves MK. Layout optimization with h-adaptivity of structures. *International Journal for Numerical Methods in Engineering* 2003; **58**:83-102.
- [3] Stainko R. An adaptive multilevel approach to the minimal compliance problem in topology optimization. *Communications in Numerical Methods in Engineering* 2006; **22**:109-118.
- [4] Wang S, de Sturler E, Paulino GH. Large-scale topology optimization using preconditioned Krylov subspace methods with recycling. *International Journal for Numerical Methods in Engineering* 2007; **69**: 2441-2468.
- [5] Wang S, de Sturler E, Paulino GH. Dynamic Adaptive Mesh Refinement for Topology Optimization. (*submitted*).

Strategies for computational efficiency in continuum structural topology: Optimization of sparse 3D systems

Colby C. SWAN* and Salam F. RAHMATALLA

*Civil and Environmental Engineering
Center for Computer-Aided Design
University of Iowa, Iowa City, Iowa USA 52242
colby-swan@uiowa.edu

Abstract

A methodology of enhanced computational efficiency is presented for continuum topology optimization of sparse structural systems. Such systems are characterized by the structural material occupying only a small fraction of the structure's envelope volume. When modeled within a continuum mechanics and topology optimization framework such structures require models of very high refinement which is computationally very expensive. The novel methodology presented here to deal with this issue is based on the idea of starting with a relatively coarse mesh of low refinement and employing a sequence of meshes featuring progressively greater degrees of uniform refinement. One starts by solving for an initial approximation to the final material layout on the coarse mesh. This design is then projected onto the next finer mesh in the sequence, and the material layout optimization process is continued. The material layout design from the second mesh can then be projected onto the third mesh for additional refinement, and so forth. The process terminates when an optimal design of sufficient sparsity, and sufficient mesh resolution is achieved. Within the proposed methodology, additional computational efficiency is realized by using a design-dependent analysis problem reduction technique. As one proceeds toward sparse optimal designs, very large regions of the structural model will be devoid of any structural material and hence can be excluded from the structural analysis problem resulting in great computational efficiency. The validity and performance characteristics of the proposed methodology are demonstrated on three different problems, two involving design of large-scale sparse three-dimensional structures for buckling stability, and the third involving design of a three-dimensional gripper compliant mechanism.

1. Introduction

There have been many attempts during the last fifteen years to use continuum topology optimization method [1] to obtain optimal forms for structures and mechanical systems. Yet, the huge computational cost involved when dealing with such problems is a main challenge in extending this method to solve problems involving highly refined finite element meshes to achieve convergent solutions with clear and smooth boundaries that reflect realistic system performances. Additionally, the material usage constraint accompanies the mesh refinement problem and could have a significant effect on the performance, weight, and shape of the resulting optimal forms in continuum topology optimization method. Up until now, this second issue has been given little attention in the literature.

One approach to achieving and dealing with fine meshes in continuum topology optimization (Maute et al. [2]) is to use adaptive mesh refinements to decrease the number of design variables and to seek smooth final topological forms. A similar approach is now extensively involved in finding optimal design forms using the evolutionary structural optimization method (ESO) [3]. In another approach, researchers enforced design symmetry during the optimization process by reducing the design space [4] by, or to remove the void nonstructural elements temporarily from the structural analysis, but reintroduce them if they needed [5,6]. The

latter approach has been shown to be very effective in dealing with problems involving geometrical nonlinearity.

The material usage constraint plays a considerable role in achieving low weight and certain performances when utilizing continuum topology optimization method. For example, most existing optimal large civil structures such as long span bridges are sparse in nature, where the real structural material occupies only a small percentage (less than 1%) of the structure's envelope volume. Therefore, in utilizing continuum structural topology optimization to obtain optimal design forms for such systems, it is crucial to impose stringent material usage constraint and implement very fine meshes in order to capture a realistic performance for such systems.

The importance of such an approach has been demonstrated in a previous work [6] where it proved to be very effective when designing structural systems for buckling instability. Similarly, it has been shown in designing hinge-free compliant mechanisms to achieve considerable flexibility [7], the amount of structural material comprising the mechanism can be progressively reduced until the desired flexibility of the mechanism is achieved. It is also crucial toward this end to use stringent material usage constraint with very fine finite element meshes

This article presents a methodology for solving large-size sparse systems in continuum structural topology design framework based on sequential refinement and size reduction strategy in a new way that is conceptually simple and theoretically sound. In sequential refinement, the proposed methodology solves a preliminary problem on a relatively coarse mesh and with a moderate material usage constraint. The resulting optimal form from this stage, the solid structural material layout, is then mapped onto a finer mesh. With a more restrictive material usage constraint, the material layout is then refined on the finer mesh. The process of optimizing the material layout and projecting it onto a finer and finer mesh while gradually tightening the material usage constraints is both efficient and robust. A size reduction strategy is implemented within each structural analysis, where the void nonstructural elements are removed temporarily but can come back quite easily and naturally if needed. The proposed size reduction technique has been tested on many linear and nonlinear systems involving geometrical nonlinearity and buckling instability and shown to be a very effective and powerful tool for reducing the computational costs, especially when dealing with sparse systems and very fine meshes.

It should be noted here that the current methodology is based on interpolation of nodal design variables using nodal basis functions [8] as opposed to element-based design variables. Although node-based design variables feature C^0 continuity, they must generally be used with perimeter constraints to achieve design convergence with mesh refinement.

2. A Brief Example

To briefly illustrate the methods being proposed, a problem is solved as shown in Fig. 1 below. The optimal layout of structural material in the circular domain is sought to carry the load at the center of the domain back to the rigid supports at the boundary of the domain. The material layout is sought to maximize the buckling stability of the resulting structure as measured by the buckling stability factor λ .

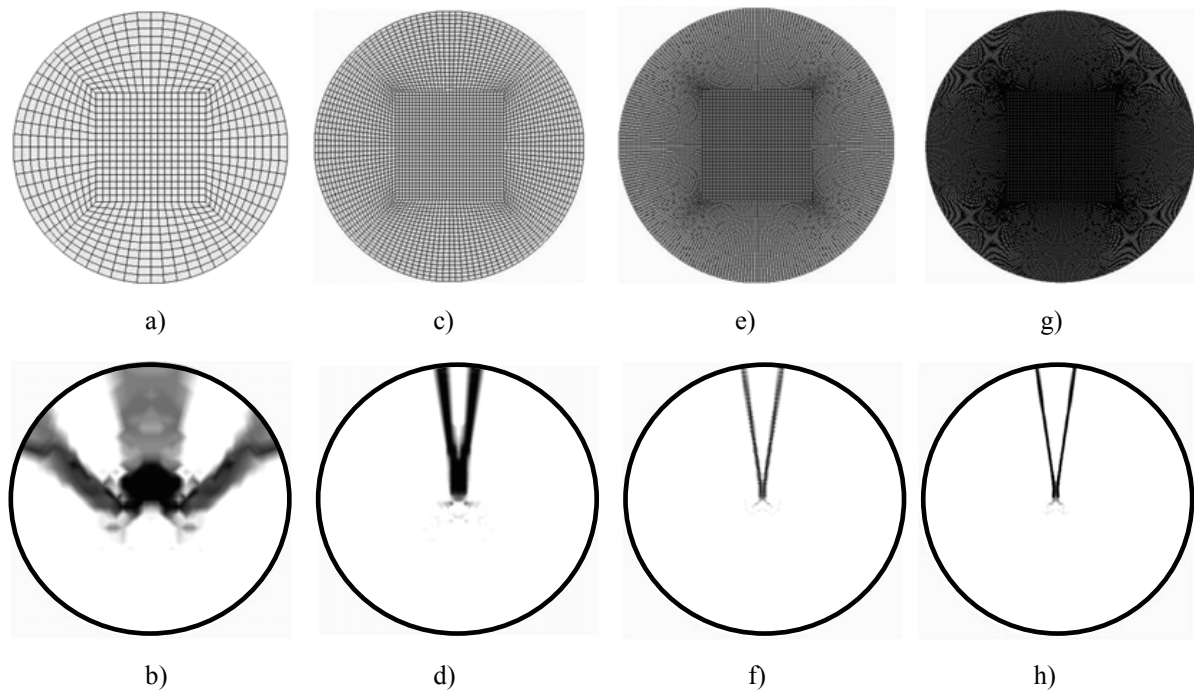


Figure 1. a) coarsest mesh of 896 elements; b) design with $V_{\text{mat}}/V_{\text{structure}}=0.20$ and $\lambda=2.17 \cdot 10^3$; c) mesh with 3,584 elements; d) material layout design with $V_{\text{mat}}/V_{\text{structure}}=0.05$ and $\lambda=1.20 \cdot 10^2$; e) mesh with 14,336 elements; f) material layout design with $V_{\text{mat}}/V_{\text{structure}}=0.015$ and $\lambda=1.00 \cdot 10^1$; g) mesh with 57,344 elements; h) material layout design with $V_{\text{mat}}/V_{\text{structure}}=0.015$ and $\lambda=1.05 \cdot 10^1$;

References

- [1] Bendsoe, M.P.; Kikuchi, N. 1988: Generating optimal topology in structural design using a homogenization method, *Comput. Meth. Appl. Mech. Engng*, 71, 197-224.
- [2] Maute, K.; Schwarz, S.; Ramm, E. 1998: Adaptive topology optimization of elastoplastic structures, *Struct. Optim.* 15, 81-91.
- [3] Bulman, S.; Sienz, J.; Hinton, E. 2001: Comparison between algorithms for structural topology optimization using a series of benchmark studies, *Computers and Structures*, 79 [12], 1203-18.
- [4] Kosaka, I.; Swan, C.C. 1999: A symmetry reduction method for continuum structural topology optimization. *Computers and Structures*, 70 [1], 47-61
- [5] Bruns, T. E.; Tortorelli, D. A. 2003: An element removal and reintroduction strategy for the topology optimization of structures and compliant mechanisms, *Int. J. Num. Meth. Engng*, 57 [10], 1413-1430.
- [6] Rahmatalla, S.; Swan, C.C. 2003: Continuum topology optimization of buckling-sensitive structures, *AIAA J.* 41 [5], 1180-1189.
- [7] Rahmatalla, S.F.; Swan, C.C., 2005: Sparse monolithic compliant mechanisms using continuum structural topology optimization, *Int. J. Num. Meth. Engng.* 62, 1579-1605
- [8] Rahmatalla, S.; Swan, C.C. 2004: A Q4/Q4 continuum structural topology optimization implementation. *Struct. Multidis. Optim.* 27, 130-135.
- [9] Rahmatalla, S.; Swan, C.C. 2003: Form-finding of sparse structures using continuum topology optimization. *J. Struct. Engng.* 129 [12], 1707-16.

Wachspress Elements for Topology Optimization

Cameron TALISCHI*, Glaucio H. PAULINO, Chau H. LE

* Department of Civil and Environmental Engineering, University of Illinois at Urbana-Champaign,
Newmark Laboratory, 205 North Mathews Avenue, Urbana, IL, 61801, U.S.A.
ktalisch@uiuc.edu

Abstract

Traditionally, standard Lagrangian-type finite elements, such as linear quads and triangles, have been the elements of choice in the field of topology optimization. However, finite element meshes with these conventional elements exhibit the well-known "checkerboard" pathology in the iterative solution of topology optimization problems. A feasible alternative to eliminate such long-standing problem consists of using hexagonal elements with Wachspress-type shape functions. The features of the hexagonal mesh include two-node connections (i.e. two elements are either not connected or connected by two nodes), and three edge-based symmetry lines per element. In contrast, quads can display 1-node connections, which can lead to checkerboard; and only have two edge-based symmetry lines. In addition, Wachspress rational shape functions satisfy the partition of unity condition and lead to conforming finite element approximations. We explore the Wachspress-type hexagonal elements and present their implementation using three approaches for topology optimization: element-based, continuous approximation of material distribution, and minimum length-scale through projection functions. Examples are presented that demonstrate the advantages of the proposed element in achieving checkerboard-free solutions and avoiding spurious fine-scale patterns from the design optimization process.

1. Introduction

Topology optimization methods seek to find the optimal layout or topology of a fixed amount of material that satisfies a required set of design demands. Despite the maturity of the field, there remains a class of numerical issues such as the well-known checkerboard problem that continues to be the focus of extensive research. This work introduces a new element for the implementation of topology optimization and demonstrates its effectiveness in removing the checkerboard pathology.

The checkerboard solutions appear as a result of inadequate or poor numerical modeling. Diaz and Sigmund [2] attributed the formation of checkerboard as a local instability to the error in the finite element approximation. The checkerboard pattern has an artificially high stiffness when modeled by lower order finite elements so it is economical in the optimization process. In a related investigation, Jog and Haber [4] addressed general numerical instabilities in topology optimization by formulating the corresponding mixed variational problem. They also concluded that insufficient interpolation of the displacement field can lead to unstable modes. Moreover, the discontinuous representation of the material field in the element-based approach (see section 3) is conducive to the appearance of checkerboard. In one approach proposed by Matsui and Terada [6], the continuity of the material field is enforced by using finite element shape functions to interpolate the density throughout the design domain from nodal densities. As a result of this choice of density field representation, the discontinuous checkerboard patches are naturally excluded from the design space. However, other forms of numerical instabilities such as "islanding" and "layering" effects have been observed with these formulations (Rahmatalla and Swan [8]).

It is evident from this discussion that the approximation of the two distinct fields of displacement and density greatly influences the stability of the topology optimization problem. In this work, we address the checkerboard issue by introducing the Wachspress hexagonal element which possesses desirable characteristics in

representing both fields (see next section). Thus, checkerboard-free solutions are obtained without any further restrictions or filtering.

2. Features of Hexagonal Wachspress Element

If we restrict ourselves to uniform meshes, there are only three possible regular tessellations in two dimensions, namely those generated by equilateral triangles, squares, and hexagons. We recognize that the hexagonal tessellation is distinguished from the other two in that it does not allow for corner contacts (Figure 1a). Consequently, unlike triangular and quadrilateral grids, the hexagonal tessellation, by the virtue of its geometry, constrains the material layout and naturally excludes the unwanted formation of checkerboard and one-node hinges. Another appealing feature of the hexagonal element is that it has more lines of symmetry per element compared to the triangular and square elements and, consequently, suffers from less directional constraint and allows for a more flexible arrangement of the final layout in the optimization process (Figure 2b).



Figure 1: An illustration of the geometric properties of the hexagonal element

In this work, we adopt Wachspress rational interpolation functions for the proposed hexagonal element. Wachspress interpolants were developed using concepts of projective geometry and are the lowest order functions that satisfy the conditions of boundedness, linear precision, and global continuity (Sukumar and Malsch [9]). The geometric construction of these shape functions is based on the algebraic equations of the edges of the polygonal domain and can be found in Wachspress [11].

3. Topology Optimization Formulation

The performance of the proposed hexagonal element is assessed through the implementation of benchmark compliance minimization problems. Using material “density” ρ as the design variable, the minimum compliance problem in the discrete form is formulated as (Bendsøe and Sigmund [1]):

$$\begin{aligned} \min_{\rho, \mathbf{u}}: \quad & c(\rho, \mathbf{u}) = \mathbf{f}^T \mathbf{u} \\ \text{s. t. :} \quad & \mathbf{K}(\rho) \mathbf{u} = \mathbf{f} \\ & \int_{\Omega} \rho dV \leq V_s \end{aligned} \quad (1)$$

Here $c(\rho, \mathbf{u})$ is the objective function (i.e. the compliance of the structure) and \mathbf{f} and \mathbf{u} are the global force and displacement vectors. Moreover, \mathbf{K} represents the global stiffness matrix, which is dependent on the density distribution. The parameter V_s is the specified maximum volume of structural material. In order to solve this optimization problem, we must choose a proper discretization of the design field. We consider the following three different approaches for implementation of the Wachspress hexagonal element:

3.1 Element-Based Approach

In the element based approach, a uniform density parameter ρ_e is assigned to each displacement finite element. The element densities become the design variables, and their sensitivities are calculated using the adjoint method:

$$\frac{\partial c}{\partial \rho_e} = -\mathbf{u}_e^T \frac{\partial \mathbf{K}_e}{\partial \rho_e} \mathbf{u}_e = -p \rho_e^{p-1} \mathbf{u}_e^T \mathbf{K}_e^0 \mathbf{u}_e \quad (2)$$

As discussed previously, the element-based implementation using linear triangular and bilinear quadrilateral displacement elements suffer from the checkerboard.

3.2 Continuous Approximation of Material Distribution (CAMD)

Alternatively, we can define the design parameters to be the nodal densities, from which the density through the domain is interpolated. Based on the concept of graded elements (Kim and Paulino [5]), we use shape functions to obtain the density within the each element and subsequently throughout design domain:

$$\rho(\mathbf{x}) = \sum_{e=1}^n \sum_{i=1}^6 N_i^e(\mathbf{x}) \rho_i^e \quad (3)$$

Here ρ_i^e denotes the nodal density of element e , which is taken to be coincident with the corresponding displacement node. This approach for topology optimization is referred to as the Continuous Approximation of Material Distribution (CAMD) (Matsui and Terada [6]). The sensitivities of the objective function with respect to the nodal densities in the CAMD implementation can be computed as follows:

$$\frac{\partial c}{\partial \rho_i^e} = - \sum_{e \in S_i} \mathbf{u}_e^T \frac{\partial \mathbf{K}_e}{\partial \rho_i^e} \mathbf{u}_e \quad (4)$$

Here S_i is the set of all elements sharing node i . If we let \mathbf{B} denote the strain-displacement matrix and \mathbf{E}^0 the constitutive matrix of the solid phase, then the sensitivity of the element stiffness matrix is given by:

$$\frac{\partial \mathbf{K}_e}{\partial \rho_i^e} = \int_{\Omega_e} p N_i^e \left(\sum_{j=1}^6 N_j^e \rho_j^e \right)^{p-1} \mathbf{B}^T \mathbf{E}^0 \mathbf{B} d\Omega \quad (5)$$

3.3 Projection Method: A minimum length-scale approach

The other scheme explored in this work is the use of projection functions with a fixed length scale. Proposed by Guest et al. [3] for Q4 discretization, the method assigns to each element a uniform density based on a projection of nodal densities surrounding that element. By choosing a fixed radius r_{min} independent of the mesh, one can obtain mesh-independent designs with prescribed minimum member size. The element density is given by a weighted average of nodal densities that are within radius r_{min} from the centroid of that element:

$$\rho_e = \frac{\sum_{i \in S_e} w_i \rho_i}{\sum_{i \in S_e} w_i} \quad (6)$$

The linear weight functions are given by (here r_i is the distance of the node i from the centroid of element e):

$$w_i = \frac{r_{min} - r_i}{r_{min}}, \quad r_i \leq r_{min} \quad (7)$$

4. Results and Conclusions

The benchmark MBB-beam problem (Olhoff et al. [7]) is solved using the Wachspres hexagonal element and results are compared with the corresponding Q4 implementation. We have solved the optimization problem using the Method of Moving Asymptotes (MMA) developed by Svanberg [10], along with a continuation on the SIMP penalty parameter. Coarse and fine meshes (with mesh sizes 60×20 and 120×40 respectively) were implemented for both elements.

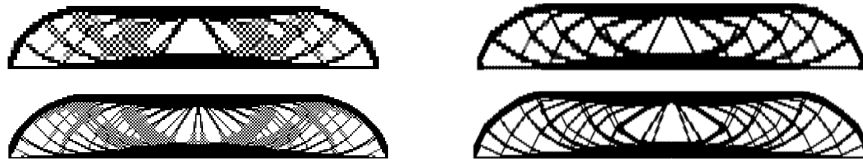


Figure 2. MBB beam design with element-based formulation: Q4 (left) and Wachspres (right) implementation

In Figure 2, the results of the element-based formulation for the Q4 element and the hexagonal element are shown. The solutions with Q4 implementation contain patches of checkerboard while no such fine scale patterns

are observed with the Wachspress implementation. Note that no filtering technique or density gradient was imposed and thus the checkerboard-free property of the hexagonal element is attributed essentially to its geometric features and interpolation characteristics. The CAMD results in Figure 3 shows that Q4/Q4 designs suffer spurious islanding and layering patterns, which are absent in designs with Wachspress elements:

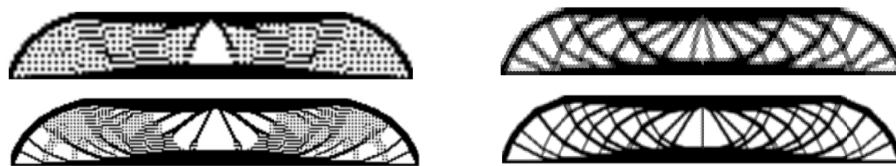


Figure 3. MBB beam design with CAMD formulation: Q4/Q4 (left) and H6/H6 (right) implementation

Finally, the results using projection scheme are presented in Figure 4. The radius of the projection r_{min} is taken to be 0.15 of the height of the beam and independent of the mesh size. We can see that despite the change in the level of mesh refinement, the same design is recovered. The length scale imposed on the optimization through r_{min} guarantees mesh-independent solutions that satisfy the required minimum member size.



Figure 4. MBB beam design with projection scheme and Wachspress hexagonal element. Note that the designs with coarse mesh (left) and fine mesh (right) are identical unlike the other two approaches.

Acknowledgement

We acknowledge the support by the Department of Energy Computational Science Graduate Fellowship Program of the Office of Science and National Nuclear Security Administration in the Department of Energy under contract DE-FG02-97ER25308. We are grateful to Prof. Krister Svanberg for providing his MMA (Method of Moving Asymptotes) code, which was used to generate the examples in this paper.

References

- [1] Bendsøe, M.P., & Sigmund, O. (2003). *Topology Optimization—Theory, Methods and Applications*. Berlin: Springer
- [2] Diaz, A., & Sigmund, O. (1995). Checkerboard patterns in layout optimization. *Structural Optimization*, 10, 40-45.
- [3] Guest, J., Prevost, J., & Belytschko, T. (2004). Achieving minimum length scale in topology optimization using nodal design variables and projection functions. *International Journal for Numerical Methods in Engineering*, 61, 238-254.
- [4] Jog, C.S., & Haber, R.B. (1996). Stability of finite element models for distributed-parameter optimization and topology design. *Computer Methods in Applied Mechanics and Engineering*, 130, 203-226.
- [5] Kim, J., & Paulino, G.H. (2002). Isoparametric graded finite elements for nonhomogeneous isotropic and orthotropic materials. *Journal of Applied Mechanics -Transactions of the ASME*, 69 (4), 502-514.
- [6] Matsui, K., & Terada, K. (2004). Continuous approximation of material distribution for topology optimization. *International Journal for Numerical Methods in Engineering*, 59, 1925-1944.
- [7] Olhoff, N., Bendsøe, M.P., & Rasmussen, J. (1991). On CAD-integrated structural topology and design optimization. *Computer Methods in Applied Mechanics and Engineering*, 89, 259-279.
- [8] Rahmatalla, S.F., & Swan, C.C. (2004). A Q4/Q4 continuum structural topology optimization. *Structural and Multidisciplinary Optimization*, 27, 130-135.
- [9] Sukumar, N., & Malsch, E.A. (2005). Recent advances in the construction of polygonal finite element interpolants. *Archives of Computational Methods in Engineering*, 11, 1-38.
- [10] Svanberg, K. (1987). The method of moving asymptotes—A new method for structural optimization. *International Journal for Numerical Methods in Engineering*, 24, 359-373.
- [11] Wachspress, E.L. (1975). *A Rational Finite Element Basis*. New York: Academic Press.

Topology optimization technique considering both static and dynamic characteristics of the structures

S.J. LEE*, J.E. BAE

*ADOPT Research Group, Department of Architectural Engineering, Gyeongsang National University
900 Gajwa-dong Jinju, Gyeongsang-namdo, Korea
lee@gnu.ac.kr

Abstract

3D topology optimization technique is described for both static and dynamic problems. The enhanced assumed strain lower order solid finite element is adopted to produce accurate structural responses such as stresses, natural frequencies and strain energies. The linearly combined function of elastic and modal strain energy terms is employed as the objective function. Therefore, the strain energy based resizing algorithm is consistently adopted to deal with both static and dynamic problems. The initial volume of structures is introduced as the constraint function. The constraint adaptive topology algorithm (CATO) is adopted to redistribute the materials in structures. The artificial material model is adopted to produce clearer and more distinct structural topologies. The material is characterized by a density parameter that is defined in terms of the volume of the voided zone, which assume as the cube cell that is centrally placed in the solid finite element. The capability of the proposed technique is tested with shell topology optimization problem. The multi-objective problems considering both elastic and modal strain energies are tackled and some meaningful observations in the material redistribution of the structure against external loads and self-vibrations have been possibly achieved. From the numerical results, it is found to be that the proposed techniques is very useful to find optimum topologies and the final optimum topologies have also been greatly affected by the consideration of the dynamic characteristics of the structures.

1. Introduction

Structural topology optimization has been studied in many ways over the last twenty years and it now became a popular method in design optimization process. There are two main issues such as material model and resizing algorithm in topology optimization. In choosing the material model, one of the important features that should be considered is that it should allow the density of material to cover the whole range of values from zero (void) to one (solid). In addition the material description should fit the periodicity assumption and should be defined by only a few parameters which are used as the design variables in the optimization algorithm. Apart from the material, another issue in topology optimization is the algorithm used to update the hole size. The optimality criteria methods have been used in popular since they can deal with many design variables without particular difficulties (Bensøe and Kikuchi [1]). On the other hands, mathematical programming methods are gradually becoming a more popular means of updating the material density parameter (Tenek and Hagiwara [2]). For example, a problem having a thousand design variables has been successfully handled using mathematical programming. However, the resizing algorithm based on the optimality criteria has still a great advantage to deal with many design variables in topology optimization. Several alternatives such as the hard-kill, the soft-kill and the evolutionary method (Xie and Steven [3]) can be used for various engineering problems.

Recently, the so-called CATO algorithm (Bulman and Hinton [4]) has also emerged and some numerical results are provided for 2D problems. It has been mostly applied to static problems and the applications of topology optimization technique into the dynamic problem are limitedly available in the open literature. Besides, the 3D topology optimization results obtained from considering both static and dynamic characteristics of the structures are very few in the previous research works. Therefore, a 3D topology optimization technique based on CATO

algorithm is described here to find the optimum topologies of the structures with simultaneous consideration of static and dynamic characteristics in design optimization process.

2. CATO Algorithm

The key aspect of the CATO has the constraint preserving the initial volume, which does not exist in the kill method. The CATO algorithm provides a means of updating the density parameters a_e or the material density parameter r_e . The basic algorithm of the CATO has the following steps:

- (a). Using a given volume fraction, calculate the initial value of design variables which are the density parameter a_e
- (b). Evaluate the appropriate constitutive properties using an artificial material model considering the current density parameter a_e
- (c). Calculate the displacements u
- (d). Calculate the strain energies U_e
- (e). Update design variables
 - (e.1) Order the elements according to their stain energy density values
 - (e.2) From a specified volume preserving relationship $\Delta a_e^k(f_e)$ evaluate the change of the density parameters Δa_e^k for each element and update the density parameter so that $a_e^{k+1} = a_e^k + \Delta a_e^k$
 - (e.3) Update density parameters a_e using the scheme described in Reference (Bulman and Hinton [4])
 - (e.4) Check whether new density parameters a_e are satisfied with the volume constrain
 - (e.5) If yes, go to (f). Otherwise, adjust a_e^{k+1} proportionately until the volume constraint is satisfied and then it is satisfied, go to (f)
- (f). Filtering the design variables if lower order finite element is used (Youn and Park [5])
- (g). If the termination criterion (Lee *et al.* [6]) is satisfied, stop. Otherwise, repeat (b)-(f)

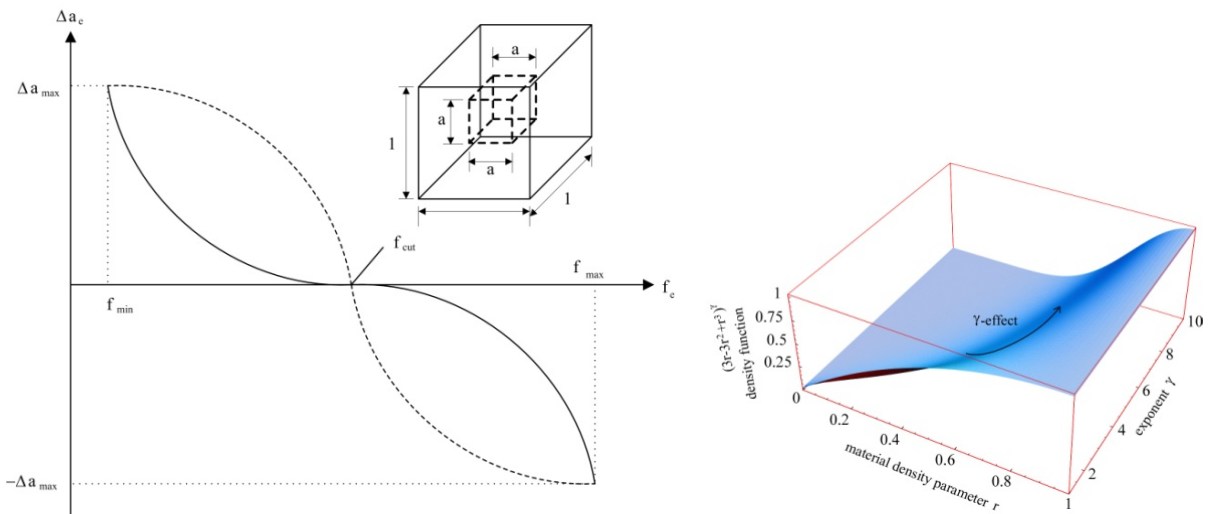


Figure 1: (Left) The relationship $\Delta a_e^k(f_e)$ at an early stage (solid line) of topology optimization iteration and at an intermediate stage (dash line); (Right) Artificial material model (Lee *et al.* [6]).

Specifically, The CATO algorithm uses an incremental relationship $\Delta a_e^k(f_e)$ to adjust the elemental density parameter a_e according to the strain energy density value f_e of each finite element. A special feature of this relationship is that it is chosen so as to preserve the total volume of the structure during the iterative optimization process. The details of such an updating scheme can be found in Reference (Bulman and Hinton [4]). Here, we will briefly describe the procedure they proposed. Figure 1 shows an example of this relationship at two stages of the scheme. The function is composed of a curve of the form $y = n^{P_{cur}}$.

3. Strain energy

The strain energy term of the structures is calculated with an enhanced lower order solid finite element and the detailed formulation of the adopted solid finite element is described in Reference (Simo *et al.* [7]). In the optimization process, we use linearly combined strain energy term of elastic and modal strain energies.

Total strain energy term for the problem considering m -load and n -natural frequency cases are defined by the following form:

$$U = \sum_{i=1}^m \lambda_i U^i + \sum_{k=1}^n \lambda_k \tilde{U}_m^k, \quad \lambda_i, \lambda_k > 0 \quad (1)$$

where U^i , \tilde{U}_m^k are the elastic strain energy for i^{th} load case and the modal strain energy (Lee and Bae [8]) induced by the k^{th} eigenvector associated with the k^{th} natural frequency such as

$$U^i = \left[\sum_{e=1}^{nel} \frac{1}{2} \int_V \boldsymbol{\varepsilon}_e^T \mathbf{D} \boldsymbol{\varepsilon}_e dV \right]^i \quad \text{and} \quad U_m^k = \left[\sum_{e=1}^{nel} \frac{1}{2} \int_V \phi_e^T \mathbf{K}_e \phi_e dV \right]^k \quad (2)$$

where $\boldsymbol{\varepsilon}$ is strain vector and \mathbf{D} is the rigidity matrix, ϕ_e is the eigenvector associated with element e and the λ_i, λ_k are the associated weights for two strain energy terms U^i, \tilde{U}_m^k respectively.

4. Free form shell

A free form shell subjected to a central point load is optimized. The geometry of the shell is expressed by the equation:

$$z = \frac{C(x^2 + y^2)}{(L/2)^2}$$

in which $C=L/10$ and $L=6$.

The four corners of the shell are clamped. The material properties used in this example are assumed to be: elastic modulus $E = 3.2 \times 10^7 \text{ N/m}^2$, Poisson's ratio $\nu = 0.3$ and the thickness of shell is $h=0.2m$. All units are assumed to be consistent.

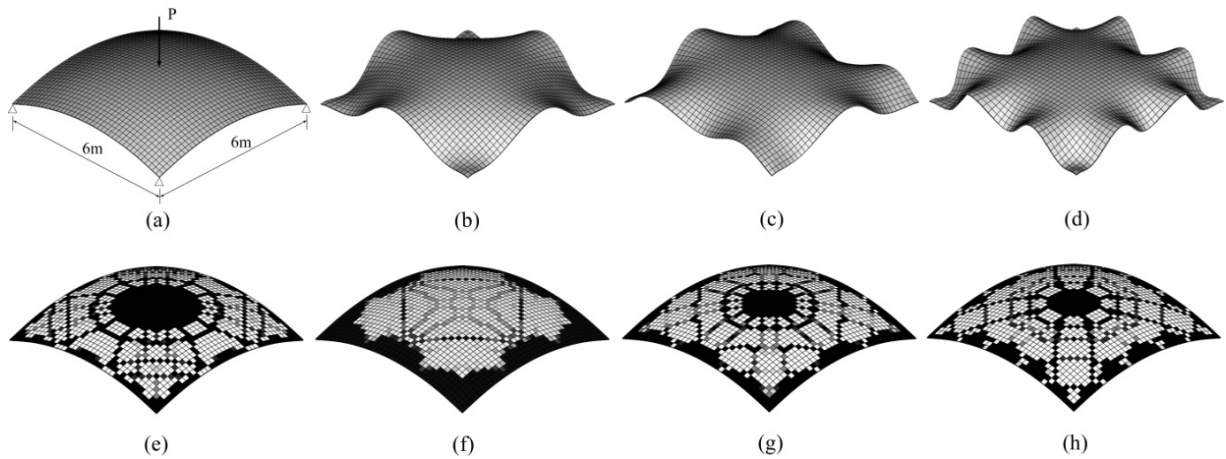


Figure 2: Free formed shell. (a) geometry, (b) the first mode shape, (c) the second mode shape (d) the third mode shape; Optimum topologies for doubly curved shell. (e) point load, (f) the first mode shape, (g) point load and the first mode shape (h) point load and the third mode shape

A mesh of 400, 8-node solid element is used for the finite element analysis in a symmetric quadrant. A volume fraction of $\Omega = 50\%$ is used and the following solution parameters $p_{ini}=5.0$, $iter=0.025$, $\Delta a_{max} = 0.01$ are used

for CATO. The tolerance of the volume fraction is 0.001. In this test, 250 iterations are allowed and the filtering process is applied until 150 iterations.

In this test, the multi-objective problem is tackled and therefore the external load $P = 10kN$ and natural mode shape shown in Figure 2 are simultaneously considered in topology optimization process. Four cases are considered: (a) P , (b) ω_1 , (c) $P + \omega_1$, (d) $P + \omega_3$. In the first case, we try to obtain the optimum topology against a central point load and the modal strain energy minimization is tried in the second case. Furthermore, multi-objective problems are considered in the other cases. Figure 2 provides the optimum topologies through the single-objective and multi-objective cases. Note that for the multi-objective problems, the elastic and modal strain energies are normalized and the uniform weight are used in the linearly combined strain energy term. From numerical results, it is observed that the material of shell has been re-distributed to form a discrete structure to resist the deformation created by external load or/ and the natural mode shapes. The values of 82%, 81%, 70%, 72% total strain energy reduction are achieved for four cases. It is found to be that the final optimum topologies have been greatly affected by the consideration of the dynamic characteristics of the structures with the use of modal strain energy.

5. Conclusions

A 3D topology optimization technique based on CATO algorithm is described in this paper. It is found to be that the present topology optimization technique is highly applicable to the design optimization problem trying to minimize both elastic and modal strain energies. In other words, simultaneous consideration of both static and dynamic characteristic of the structure is successfully achieved in design optimization process. We also see the possibility of using modal strain energy as a single load case in the framework of multi-load case problems.

Acknowledgement

The research grants from the Ministry of Construction & Transportation, Korea, for the Construction Technology Research & Development Program (C105A1020001-05A0502-00112) are gratefully acknowledged.

References

- [1] Bensøe MP and Kikuchi N. Generating optimal topologies in structural design using homogenization method. *Computer Methods in Applied Mechanics and Engineering* 1998; **71**: 197-224.
- [2] Tenek LH and Hagiwara I. Static and vibrational shape and topology optimization using homogenization and mathematical programming. *Computer Methods in Applied Mechanics and Engineering*, 1993; **109**: 143-154.
- [3] Xie YM and Steven GP. *Evolutionary Structural Optimization*, Springer-Verlag, 1997.
- [4] Bulman SD and Hinton E. Constrained adaptive topology optimization of engineering structures. *Design Optimization* 1999; **1**: 419-439.
- [5] Youn SK and Park SH. A study on the shape extraction process in the structural topology optimization using homogenization material. *Computers & Structures* 1997; **62**: 527-538.
- [6] Lee SJ, Bae JE and Hinton E. Shell topology optimization using layered artificial material model. *International Journal for Numerical Methods in Engineering* 2000; **47**: 843-867.
- [7] Simo JC, Armero F and Taylor RL. Improved versions of assumed enhanced strain tri-linear elements for three-dimensional finite deformation problems. *Computer Methods in Applied Mechanics and Engineering* 1993; **110**: 359-386.
- [8] Lee SJ and Bae JE. The strain energy based topology optimization technique maximizing the fundamental frequency of the structures. In *Proceedings of the 10th East Asia-Pacific Conference on Structural Engineering & Construction (EASEC-10): Analytical and Computational Methods* 2006; 229-234.

Topology Optimization Method utilizing iterative solvers with subspace recycling applied to high-resolution Electrical Impedance Tomography

Luís Augusto MELLO*, Emílio Carlos Nelli SILVA, Eric de STURLER, Gláucio Hermógenes PAULINO

*Department of Mechatronics and Mechanical Systems Engineering, University of São Paulo
Av. Professor Mello Moraes, 2231, Office number: MZ-14, São Paulo, SP, 05508-900, Brazil
luis.mello@poli.usp.br

Abstract

Electrical Impedance Tomography (EIT) images internal objects within a body. Electrodes are attached to the boundary of the body, low intensity alternated currents are applied and the resulting electric potentials are measured. Then, an estimation algorithm obtains the three-dimensional (3D) internal admittivity distribution, which corresponds to the image. One of the main goals of EIT is to achieve high resolution and low computational time, which are related quantities. In this paper, a fast iterative solver based on the recycling of approximate invariant subspaces is proposed in order to reduce the time employed to obtain finite element solutions (the typical bottleneck in EIT), for a given resolution. Additionally, the Topology Optimization Method (TOM) is proposed to obtain the admittivity distribution. Results obtained show the effectiveness of our approach and relatively high resolutions (the mesh has 267.051 elements, 53.692 nodes and 53.691 degrees of freedom) at small computational time (approximately 6 hours), even on a standard PC.

1. Introduction

EIT finds the admittivity (conductivity and permittivity) distribution in a given model of a body which reproduces the boundary measurements of currents and potentials on electrodes attached to that body (Mello *et al.* [4]). The admittivity distribution represents the solution of a non-linear and ill-posed inverse problem. Several combinations of current-carrying electrodes can be chosen and, therefore, many induced electric potential values may be available for the admittivity estimation, which is meant to reduce the solution space.

EIT applications range from medical to industrial. In medical applications, it is applied to detect breast cancer and to monitor lung aeration (Mello *et al.* [4]), for instance. In the last case, the main interest of our group, the reconstruction of absolute admittivity values has shown its relevance, since these absolute values allow distinguishing some lung pathologies (Mello *et al.* [4]).

Several algorithms have been proposed to solve the non-linear inverse problem for the absolute admittivity values. They are usually based on iterative methods such as Gauss-Newton or TOM (Mello *et al.* [4]). The Finite Element Method (FEM) is frequently employed to model the body, which means that linear systems must be solved. Since several combinations of current-carrying electrode are considered, the linear systems have different right-hand sides. Iterative solvers are usually reported rather than direct methods due to relatively low storage requirements and fast computations, even for multiple right-hand sides (see Vorst [5]).

One of the main goals of EIT is to achieve high resolution at low computational times. However, when the resolution is increased, which is carried out by refining the finite element mesh, the computational time is also increased, especially in the case of 3D meshes. Therefore, there is a trade-off between the element size and the time spent to obtain an image in EIT and, in fact, the time can be prohibitive in a practical 3D case.

In this work, we employ a relatively new technique (Wang *et al.* [6]) to reduce the EIT computation time for a constant resolution and, therefore, we address the trade-off issue. The technique is called recycling and is

applied to diminish the time and number of iterations of each FEM solution, the bottleneck of the admittivity estimation. We employ TOM to solve the inverse problem, a method that has presented relatively good results (Mello *et al.* [4]). TOM combines the Sequential Linear Programming (SLP) and FEM to find the properties distribution which optimizes an objective function subjected to constraints. The recycling technique utilizes the fact that the changes in the matrices of the linear systems during the iterative optimization process are small in order to speed up the convergence of each system. In addition, the technique can be applied to the linear systems solved to compute the gradient of the objective function during one iteration. We consider the image reconstruction of a cylinder with relatively high resistivity within a conductive body. In other words, a binary (0-1) problem is solved, for which TOM is indicated (see Bendsøe and Sigmund [1]). We also simulate the data, which means that a numerical phantom (Kaipio and Somersalo [2]) provides the measured potentials.

2. FEM model

Maxwell's equations can describe the electromagnetic fields in the body, as mentioned by Kaipio and Somersalo [2]. Based on these equations and considering the quasi-static approximation for a linear and isotropic medium and a sufficiently small excitation frequency, a conductive medium is assumed and we can obtain

$$\mathbf{K}(\boldsymbol{\sigma})\mathbf{V}_j(\boldsymbol{\sigma}) = \mathbf{I}_j \quad (1)$$

which, together with Neumann's and Dirichlet's boundary conditions, corresponds to the FEM model of a typical EIT setup. Four nodes tetrahedral finite elements comprise the FEM mesh and $\boldsymbol{\sigma}$ is the vector of element conductivities, $\mathbf{K}(\boldsymbol{\sigma})$ is the conductivity matrix and \mathbf{I}_j and $\mathbf{V}_j(\boldsymbol{\sigma})$ are the vectors of nodal electric currents and electric potentials, respectively. The index j indicates different current-carrying electrodes (for simplicity, we consider narrow electrodes, which are modeled as point electrodes at nodes).

3. TOM

The EIT inverse problem is usually based on square error function for potential values

$$F = \frac{1}{2} \sum_{j=1}^{n_e} (\mathbf{A}_j \mathbf{V}_j(\boldsymbol{\sigma}) - \mathbf{V}_{0j})^T (\mathbf{A}_j \mathbf{V}_j(\boldsymbol{\sigma}) - \mathbf{V}_{0j}) \quad (2)$$

where n_e is the number of different current-carrying electrodes, \mathbf{A}_j is a diagonal and square matrix whose values are equal to one at positions of measurement electrodes and zero otherwise, and \mathbf{V}_{0j} is the vector of measurements whose components are zero unless they represent a measurement electrode.

Following the TOM theory (see Bendsøe and Sigmund [1]), a material model is defined. In this work, the continuous approximation of material distribution by Matsui and Terada [3] is chosen, which means that the conductivity of the m -th finite element is given by

$$\sigma_m = \rho_m^p \sigma_A + (1 - \rho_m^p) \sigma_B \quad (3)$$

and depends on nodal values, varying linearly within the element in the same way as the electric potentials. In equation (4), σ_A and σ_B are the electric conductivities of the materials that compose the body and the exponent p introduces penalization into the model, which means that lower values of conductivities are favored.

Based on equations (3) and (4), we define the following optimization problem

$$\text{minimize } F(\boldsymbol{\rho}), \quad \text{subjected to } \mathbf{K}(\boldsymbol{\rho})\mathbf{V}_j(\boldsymbol{\rho}) = \mathbf{I}_j \text{ and } \mathbf{0} \leq \boldsymbol{\rho} \leq \mathbf{1} \quad (4)$$

where $\boldsymbol{\rho}$ is the vector of nodal optimization variables. The gradient of F , utilized in the SLP iteration, is given by

$$\frac{\partial F(\boldsymbol{\rho})}{\partial \rho_k} = - \sum_{j=1}^{n_e} \mathbf{V}_j^T(\boldsymbol{\rho}) \frac{\partial \mathbf{K}(\boldsymbol{\rho})}{\partial \rho_k} \mathbf{K}^{-1}(\boldsymbol{\rho}) (\mathbf{A}_j \mathbf{V}_j(\boldsymbol{\sigma}) - \mathbf{V}_{0j}). \quad (5)$$

The derivation of equation (6) is shown in detail in Mello *et al.* [4]. The equation shows that $2n_e$ linear systems have to be solved in each SLP iteration. Each solution is obtained by the solver described in the next section.

4. Solution of the Linear systems: MINRES algorithm with recycling

MINRES is a Krylov subspace method intended for solving linear systems of equations that contain a symmetric matrix (Vorst [5]). In each iteration, the three-term Arnoldi recurrence generates a new vector, updating the

orthonormal basis of the Krylov subspace. Then, an approximate solution in the Krylov subspace that minimizes the two-norm of the current residual is obtained.

The recycling version of MINRES (RMINRES) selects a subspace employed in the solution of a linear system and utilize it in the solution of the next (Wang *et al.* [6]). Therefore, it must be assured that this subspace and the corresponding subspace of the next system are close for RMINRES to be effective.

The recycled subspace is considered in the Arnoldi recurrence of the subsequent system, which means that each new vector in the recurrence has to be orthogonal to \mathbf{KU} , where the columns of \mathbf{U} contain a basis for the recycled subspace. In addition, an approximate solution in a new subspace spanned by the columns of \mathbf{U} and the Arnoldi vectors is obtained. In this work, harmonic Ritz vectors with respect to this new subspace are recycled. The harmonic Ritz vectors are good choices since they approximate eigenvectors of the matrix of the linear system.

As can be seen in equation (6), the systems differ only with respect to the right-hand sides. The RMINRES solver is utilized in these cases, reducing the number of iterations and the runtime of the linear solver. After 2ne systems are solved, the last recycled subspace is utilized in the first system of the next SLP iteration. Since the matrices of linear systems change slowly between SLP steps, the recycled subspace can reduce the number of iterations as well as the runtime of the linear solver also in these cases. Additionally, since the changes tend to diminish along the iterative process, the effectiveness of the technique is supposed to be increased towards the convergence of the optimization solution.

5. Results

In all results, the incomplete Cholesky decomposition with zero fill-in of the conductivity matrix is employed as a preconditioner (Wang *et al.* [6]). These results are obtained on a PC with an Intel® Core™ 2 Quad Q6700 2.66GHz processor, approximately 8GB of RAM and the Mandriva Linux system.

Based on the work of Wang *et al.* [6], the performance of RMINRES is studied. In the tests, the dimension of the recycled subspace (r) is varied. In this case, RMINRES is referred to as RMINRES(r). Additionally, RMINRES is compared to MINRES and to the Conjugate Gradient (CG) algorithm (Vorst [5]). The maximum dimension of the subspace kept (and hence, the maximum number of Arnoldi vectors maintained) to update the subspace which is recycled remains equal to 100.

The figure 1 shows the mesh of the numerical phantom and a typical image obtained (the peculiarities regarding the different values of r are mentioned in the following results). Thirty-two uniformly placed point electrodes are considered on the surface of the mesh. Additionally, thirty-two different current-carrying electrodes are utilized, which means that $n_e=32$. The electric currents and the exponent p are equal to 0.001mA and 1, respectively. In all cases, the electric potential in the same node is taken as ground. Also, thirty-two electric potentials are measured for each different current-carrying electrode, which means that 1.024 measurements are available. The convergence criterion is that the maximum change in the nodal optimization variables is less than 0.02. Finally, the initial values of the optimization variables are equal to one, which correspond to $4\Omega\text{m}$.

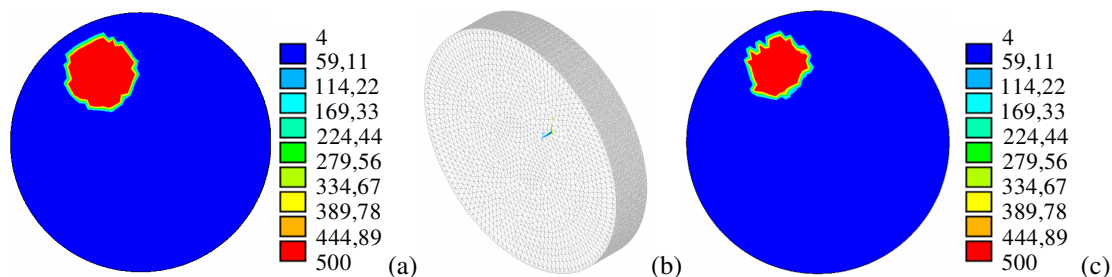


Figure 1: (a) Resistivity distribution of the numerical phantom. (b) Mesh of the phantom (53.692 nodes – 53.691 degrees of freedom – and 267.051 elements). (c) Estimated image.

The number of iterations and time spent in solving the linear system in equation (2) with $j=1$ are shown in Figure 2. It can be seen that recycling become more effective towards the end of the TOM optimization process,

as mentioned before. It also can be seen that the RMINRES is more effective than MINRES and that the effectiveness increases with r . However, there is a trade-off between the number of iterations for the solver and the computational cost per SLP iteration and, in fact, the algorithm become unsuccessful in reducing the time of each solution for $r=20$.

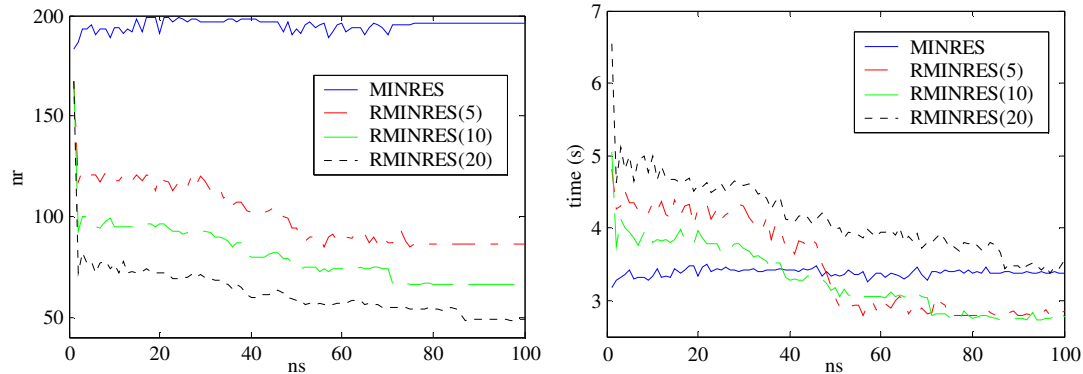


Figure 2: Number of iteration (nr) and time of RMINRES(r) for each SLP iteration (ns).

Finally, RMINRES(10) and CG are compared, the method of choice for symmetric and positive definite matrices that often arises in EIT. Again, the Cholesky preconditioner is considered. The total runtime is approximately equal to 6,67 hours for CG and 5,75 hours for RMINRES(10), showing an expressive difference.

6. Conclusion

In this work, the recycling technique was introduced in the context of EIT in order to reduce the computational cost utilized to obtain a 3D image. It was shown that for suitable size of the recycled subspace, the algorithm leads to a 28% reduction in computation time at the end of the SLP iterative process. In addition, a 13% reduction in the computation time from CG to RMINRES(10) was obtained, which shows the importance of the extension of recycling to the CG algorithm. In future works, we intend to implement other tools in order to speed up the optimization process, such as parallelization of the finite element solutions and block Krylov Methods. We also intend to consider the recycling technique in the case of CG.

Acknowledgement

The authors acknowledge Shun Wang for all the support provided regarding the RMINRES code. The first author also thank to FAPESP (The State of São Paulo Research Foundation) for his doctoral scholarship (grant number 2005/00270-1) and for the research project support (grant number: 01/05303-4). The second author acknowledges the financial support of CNPq (National Counsel of Technological and Scientific Development).

References

- [1] Bendsøe MP and Sigmund O. *Topology Optimization: Theory, Methods and Applications*. Springer-Verlag Berlin Heidelberg, 2003.
- [2] Kaipio J and Somersalo E. *Statistical and Computational Inverse Problems*. Springer Science+Business Media, Inc., 2005.
- [3] Matsui K and Terada K. Continuous approximation of material distribution for topology optimization. *International Journal for Numerical Methods in Engineering* 2004; **59**: 1925-1944.
- [4] Mello LAM, Lima CR, Amato MBP, Lima RG, Silva ECN. Three-dimensional Electrical Impedance Tomography: a Topology Optimization approach. *IEEE Transactions on Biomedical Engineering* 2008; **55**:531-540.
- [5] Vorst HA. *Iterative Krylov Methods for Large Linear Systems*. Cambridge University Press, 2003.
- [6] Wang S, Sturler E, Paulino GH. Large-scale topology optimization using preconditioned Krylov subspace methods with recycling. *International Journal for Numerical Methods in Engineering* 2007; **69**:2441-2468.

Topology optimization considering fabrication errors and length scale constraints

James K. GUEST*

*Department of Civil Engineering
Johns Hopkins University
3400 N. Charles Street
Baltimore, MD 21218
jkguest@jhu.edu

Abstract

Structural topology optimization is a powerful design tool capable of discovering new solutions to engineering design problems. Topology optimization, however, typically requires a large, discrete design space and problems must thus be simplified to become computationally tractable. Simplification often results in solutions that are physically unrealizable from a manufacturing perspective, or suboptimal when considering real-world engineering conditions and fabrication processes. This paper discusses methodologies for imposing length scales on the structural features to influence constructability, and methodologies for incorporating uncertainties arising from fabrications and construction errors. These uncertainties may result from errors in geometry and/or flaws in material properties. Specifically, a recently developed perturbation approach for modelling node location uncertainties is discussed and extended to include material property uncertainties. We then also discuss application of the technique to the design of material microstructures. It is shown that the inclusion of length scale constraints and fabrication flaws in the problem formulation can have substantial impact on the topology of optimized designs.

1. Introduction

Structural optimization is the application of formal optimization methodologies to structural design problems. The term structure herein is not limited to civil engineering-scale structures, but refers to general load-carrying topologies. The most powerful type of structural optimization is topology optimization, where the goal is to identify the optimal distribution of material within a design domain. The attraction of topology optimization is that it does not require, nor is it limited to, a predefined structural connectivity of the design space, thereby facilitating discovery of new design ideas. The cost of this design freedom is an extremely large (and often discrete) design space. This has led most researchers to focus on deterministic design problems with relatively simple governing mechanics. Loads, boundary conditions, and material properties are often assumed known. Additionally, fabrication precision is assumed to be exact and the physical structure will be identical to the proposed design. The reader is referred to Bendsøe and Sigmund [3] for a review of topology optimization.

While these assumptions make topology optimization problems tractable, they can lead to designs that are impractical and suboptimal when considering real-world engineering conditions, including uncertainties in the load and fabrication process. For example, consider the truss topology optimization problem shown in Figure 1a with a goal of maximizing stiffness. When solving this problem under linear elastic conditions, the collinear design of Figure 1b is identified as the optimal solution. However, this solution is unstable and will collapse under any perturbation in structure geometry or applied loading. This is certain to occur in engineering applications, even with tight manufacturing tolerances. Additionally, this collinear design could be susceptible to flaws in material or geometric section properties as there is no alternate load path for the structure.

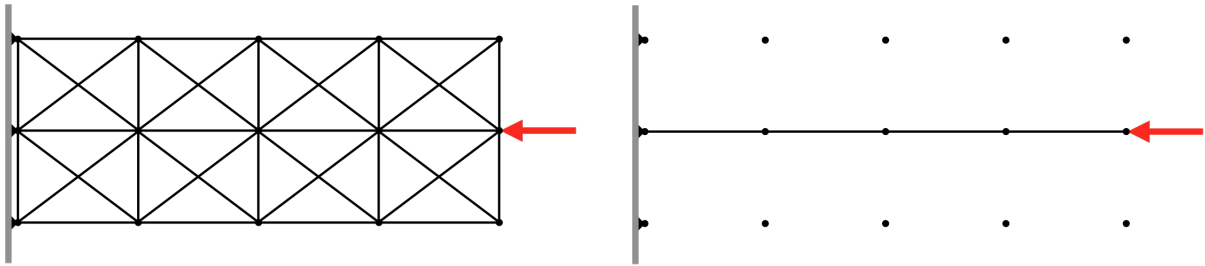


Figure 1: Maximum stiffness truss topology optimization assuming linear elastic behavior. The truss ground structure (left) and the optimal solution (right). The four members in the optimal solution have increased cross-sectional area but the resulting structure is unstable.

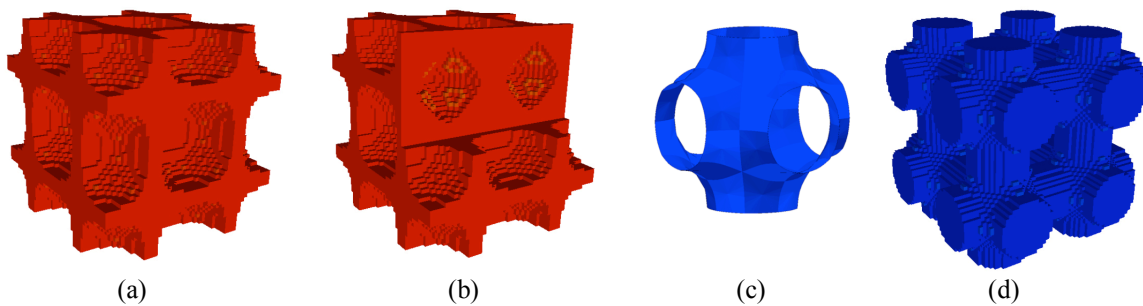


Figure 2: Examples of periodic material microstructures optimized for 50% void ratios. (a) Isotropic material with maximal bulk modulus (solid phase shown). The void spheres are arranged in a staggered pattern to achieve isotropy, as shown by cut-away in (b). (c) Schwartz P minimal surface that resembles the base cell of material with maximal isotropic fluid permeability (fluid-solid interface shown). The fluid phase of the periodic material (8 base cells) is shown in (d).

Topology optimization can also be used to design material microstructures via inverse homogenization. Here the goal is to identify microstructures that yield desired effective material properties of the bulk material. Topology optimization at this scale often leads to complex topologies composed of idealized shapes. Figures 2a-b display isotropic microstructures optimized for maximal bulk modulus. These microstructures contain spherical voids staggered in the pattern of a body-centered cubic Bravais lattice (Sigmund [9], Guest and Prévost [6]). Microstructures optimized for isotropic fluid permeability resemble triply periodic Schwartz P minimal surfaces as shown in Figure 2c-d (Guest and Prévost [6]). Such topologies are difficult to manufacture and subsequent imperfections may have dramatic impact on performance.

Practicing designers account for fabrication constraints and uncertainties informally using engineering judgment. In this paper we will discuss formulation and solution strategies for incorporating manufacturing constraints and uncertainties in topology optimization problems. These strategies are developed in the context of macroscopic design problems while extensions to periodic material microstructures are also discussed.

2. Fabrication and construction considerations

2.1 Feature length scale constraints

Maximum stiffness topology optimization problems are known to be ill-posed. Given a total volume of material, solutions can typically be improved by making holes smaller and more numerous. This leads to so-called chattering designs where the number of holes is unbounded (Haber *et al.* [8]). Such designs are unrealizable from a manufacturing point of view. When solved numerically, this property appears in the form of mesh dependencies and checkerboard patterns. A popular approach for addressing this issue is to restrict the design space by requiring structural features to attain a minimum length scale. This makes the problem well-

posed as features below this length scale are prohibited from forming. The minimum allowable length scale also directly influences manufacturing constraints and associated costs.

Minimum length scale can be imposed in truss and frame design by simply assigning lower bound on cross-sectional area. Enforcing minimum length scale in continuum design is more difficult as a structural member is defined by the union of solid elements. Several researchers have proposed techniques for imposing minimum length scale. The scheme used here is the Heaviside Projection Method (HPM) to topology optimization (Guest *et al.* [7]). HPM uses an auxiliary design variable field that is projected onto element space to define topology. This projection occurs over the minimum length scale and uses a regularized Heaviside function. Figure 3 displays designs for the simply supported beam problem found using HPM with various user-prescribed minimum length scales. Designs with smaller prescribed minimum length scales tend to be more intricate and offer improved performance under deterministic linear elastic conditions. Prescribing a larger minimum length scale produces simpler designs that are less costly to manufacture and likely less susceptible to flaws.

To control structure geometry further, it is noted that designers could also prescribe a maximum length scale using a technique recently presented in Guest [4]. This provides the designer complete control over member sizes and thus influence over manufacturability, cost, and potentially even structural performance properties such as structural redundancy.

2.2 Fabrication errors

Most topology optimization methodologies assume the structure will be constructed exactly as designed. As discussed, this can lead to impractical, unstable, and/or non-robust designs. Guest and Igusa [5] recently proposed a perturbation approach for accounting for geometric uncertainties, represented by uncertainties in the locations of the nodes of the finite element mesh. Express the inverse of the random global stiffness matrix \mathbf{K} as the sum of deterministic and random components $\mathbf{K}^{-1} = \mathbf{K}_0^{-1} + \delta\mathbf{K}^{-1}$, where \mathbf{K}_0 is the deterministic (as designed) global stiffness matrix and $\delta\mathbf{K}$ is the random component due to geometric uncertainty. For a single deterministic applied load \mathbf{f} , the expected compliance objective function becomes

$$E[\mathbf{f}^T \mathbf{d}] = \mathbf{f}^T E[\mathbf{K}(\boldsymbol{\rho})^{-1}] \mathbf{f} = \mathbf{f}^T \mathbf{K}_0(\boldsymbol{\rho})^{-1} \mathbf{f} + \mathbf{f}^T E[\delta\mathbf{K}(\boldsymbol{\rho})^{-1}] \mathbf{f} \quad (1)$$

It was shown that when fabrication error is small in relation to structural member length scale, (1) can be reformulated as a random loads problem. The equivalent random loads $\delta\mathbf{f}$ are of the form $\delta\mathbf{f}_j = \sigma_j \mathbf{Q}_j \mathbf{d}$, where \mathbf{Q}_j are based on first and second derivatives of the global stiffness matrix and \mathbf{d} are the displacements under the deterministic applied load \mathbf{f} . These random forces thus depend on the current structural configuration and response and evolve simultaneously with the progression of the structural design throughout the optimization.

Using the equivalent random loads approach, the expected compliance objective function is written as

$$\min_{\boldsymbol{\rho}} E[\mathbf{f}^T \mathbf{d}] = \mathbf{f}^T \mathbf{K}_0(\boldsymbol{\rho})^{-1} \mathbf{f} + \sum_j \delta\mathbf{f}_j^T \mathbf{K}_0(\boldsymbol{\rho})^{-1} \delta\mathbf{f}_j \quad (2)$$

which closely resembles the discrete random loads formulation frequently solved in literature (Ben-Tal and Nemirovski [1]; Bendsøe *et al.* [2]). The reader is referred to Guest and Igusa [5] for the derivations and the details regarding computationally efficient forms of and solution algorithms for (2). Herein we note that only the deterministic global stiffness matrix appears in (2) and the resulting optimization problem. Therefore, as the primary computational expense is in solving the equilibrium equations, the added expense in solving the random nodes problem here is limited to the addition of multiple right-hand sides.

Considering fabrication errors in the design formulation can have a dramatic affect on optimal designs as illustrated by Figure 4. Under deterministic conditions, topology optimization of the ground structure in Figure

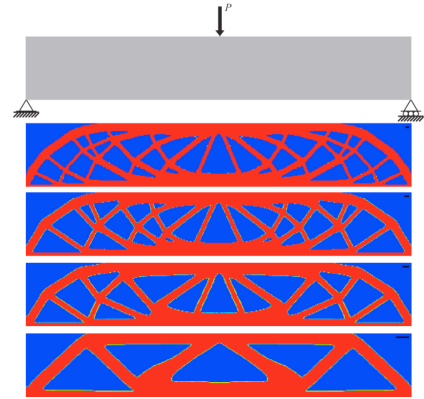


Figure 3: Maximum stiffness designs for a simply supported beam loaded at midspan (top). The prescribed minimum length scale (shown by black bars) increases from top to bottom. The designer has control over member sizes and consequently influence over manufacturability, cost, and sensitivity to flaws.

4a results in the unstable truss structure of Figure 4b. The vertical posts over the supports and top truss chord are unbraced compression members. This structure is clearly unstable and will fail once load is applied and deformation occurs. It is noted that 2nd order analysis is required to capture this instability. When node location uncertainties are considered, topology optimization yields the braced truss structure of Figure 4c. This structure is stable and more robust, despite considering only first order behavior.

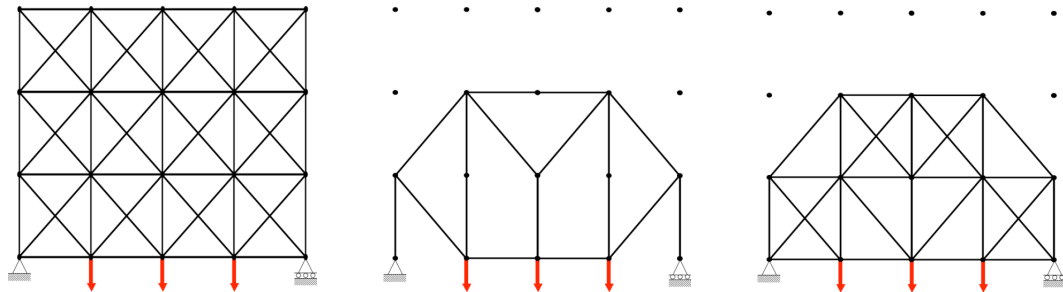


Figure 4: Initial truss ground structure (left) for the maximum stiffness topology optimization design problem. If fabrication errors are not considered, the optimization leads to an unstable design (center). A stable, more robust design (right) results when the potential for fabrication errors are incorporated into the topology optimization formulation.

2.3 Extension to material microstructures

Topology optimization can also be used to design material microstructures. This is an inverse homogenization problem where the goal is to identify microstructures that yield desired effective material properties at the macroscale. Fabrication uncertainties can be incorporated into the microstructural optimal design problem by applying the perturbation methodology to the homogenization equations used to estimate properties of the bulk material. A complication of (2) over the standard multiple loads problem is that the equivalent random loads are functions of deterministic response. The technique is further complicated here by the homogenization load cases (the applied unit test strain fields). First, there are multiple load cases (3 in 2-d and 6 in 3-d). Second, the loads are dependent upon the microstructural design. Although the resulting equations are cumbersome and are omitted here for brevity, recent work has shown that the solution of these equations is straightforward.

References

- [1] Ben-Tal A and Nemirovski A. Robust truss topology design via semidefinite programming. *SIAM Journal of Optimization* 1997; **7**:991–1016.
- [2] Bendsøe MP, Ben-Tal A, and Zowe J. Optimization methods for truss geometry and topology design. *Structural Optimization* 1994; **7**:141-159.
- [3] Bendsøe MP and Sigmund O. *Topology Optimization: Theory, Methods, and Applications*, Springer, 2003.
- [4] Guest JK. Imposing maximum length scale in topology optimization. *Structural and Multidisciplinary Optimization*, in press.
- [5] Guest JK and Igusa T. Structural optimization under uncertain loads and nodal locations. *Computer Methods in Applied Mechanics and Engineering*, in press.
- [6] Guest JK and Prévost JH. Optimizing multifunctional materials: Design of microstructures for maximized stiffness and fluid permeability. *International Journal of Solids and Structures* 2006; **43**:7028-7047.
- [7] Guest JK, Prévost JH, and Belytschko T. Achieving minimum length scale in topology optimization using nodal design variables and projection functions. *International Journal for Numerical Methods in Engineering* 2004; **61**:238-254.
- [8] Haber RB, Jog CS, Bendsøe MP. A new approach to variable-topology shape design using a constraint on perimeter. *Structural Optimization* 1996; **11**:1-12.
- [9] Sigmund O. A new class of extremal composites. *Journal of Mechanics and Physics of Solids* 2000; **48**: 397-428.

A simple and effective inverse projection scheme for void distribution control in topology optimization

Glauco H. PAULINO*, Sylvia ALMEIDA, Emilio SILVA

*University of Illinois at Urbana-Champaign – Department of Civil and Environmental Engineering
Newmark Laboratory, 205 North Mathews Avenue, Urbana, IL 61801, USA
paulino@uiuc.edu

Abstract

The ability to control both the minimum size of structural members and the maximum size of the holes are essential requirements in the topology optimization design process for manufacturing. This paper addresses both requirements by means of a unified approach involving mesh-independent projection techniques. A standard direct projection scheme is used to control the minimum length of structural members, while an inverse projection is developed to control the minimum hole size. An example demonstrates features of the direct and the inverse projection techniques.

1. Introduction

Engineers aim at improving the structural optimization process so as to find an effective answer to the problem of automatic design of structural components. Although optimization techniques can play a role in several stages of the design process, the state of the art does not allow a complete automation yet. Some techniques, such as parameter optimization, are more suited to the final stages of the design process because they can easily incorporate limit state constraints. On the other hand, topology optimization including material distribution fits better in the initial stages of the design process.

Achieving control of manufacturing design and considering limit state constraints are some of the most important issues to make topology optimization more than a preliminary design tool. Controlling the structural member sizes and the minimum size of holes are just two of several manufacturing requirements that must be observed in the design process. Techniques to avoid numerical instabilities in the topology optimization process also provide an indirect control over the resulting structural member sizes. For instance, the weighted average over element densities adopted in most density filters (Bourdin [1]), and the weighted average over sensitivities adopted in the sensitivity filters (Sigmund [4] and [5]), increase the structural member size as the dimension of the filter is increased. Guest *et al* [3] presented a mesh-independent projection scheme to achieve minimum length scale on structural members obtained by means of topology optimization. This scheme has been extended to a multiphysics setting by Carbonari *et al*. [2].

The approach introduced in this paper addresses the problem of imposing a minimum size of the holes using an inverse projection scheme. The details of the method are given below.

2. Review of the direct projection scheme

Guest *et al*. [3] proposed a mesh-independent projection scheme to achieve minimum length scale on structural members generated by topology optimization. The nodes inside a circular region Ω_w^e in the neighborhood of the element of reference are included in the evaluation of the element density ρ^e used in the finite element analysis (Figure 1a). The set of nodes S_w^e to be projected are defined by

$$\mathbf{x}_j \in S_w^e \quad \text{if} \quad r_j^e = |\mathbf{x}_j - \mathbf{x}^e| \leq r_{\min} \quad (1)$$

where \mathbf{x}_j are the coordinates of the node j , \mathbf{x}^e are the coordinates of the center of the element, and r_j^e is the distance between the center of the element e and the node j . The projection consists essentially of a cone of base $2 r_{min}$ and unit height centered at the center of the element (Figure 1b).

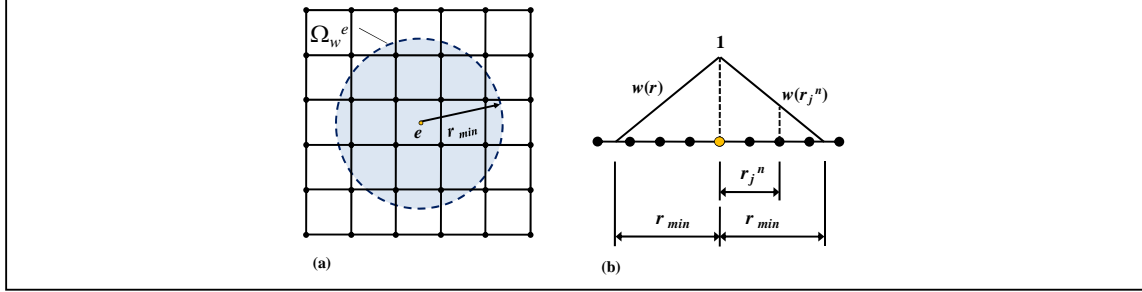


Figure 1: Direct projection scheme: (a) domain Ω_w^e ; (b) linear weight function

Moreover, the following relationships are employed (see Figure 1):

$$\rho^e = \frac{\sum y_j w(\mathbf{x}_j - \mathbf{x}^e)}{\sum w(\mathbf{x}_j - \mathbf{x}^e)} \quad (2)$$

$$w(\mathbf{x}_j - \mathbf{x}^e) = \begin{cases} \frac{r_{min} - r_j^e}{r_{min}} & \text{if } x_j \in \Omega_w^e \\ 0 & \text{if } x_j \notin \Omega_w^e \end{cases} \quad (3)$$

The nodal variables y_j are weighted to evaluate the element volume fraction ρ^e of element e , as shown in (2), using the linear weight function defined in (3). Other functions can be used as well (see Guest *et al.* [3]).

The weight function (3) is mesh-independent because r_{min} is an invariant length scale, however, the number of nodes evaluated in the weight function increases as the mesh is refined. The radius r_{min} is a physical length scale, which imposes that the minimum allowable member size corresponds to $2 r_{min}$, the basis of the projection cone.

3. The proposed inverse projection scheme

We propose a similar scheme to obtain the minimum size of holes in the topology using an inverse projection. The projection scheme is defined in a circular region Ω_{inv}^e in the neighborhood of the element (Figure 2a). The set nodes S_{inv}^e in the Ω_{inv}^e region are defined by

$$\mathbf{x}_j \in S_{inv}^e \quad \text{if} \quad r_j^e = |\mathbf{x}_j - \mathbf{x}^e| \leq r_{inv} \quad (4)$$

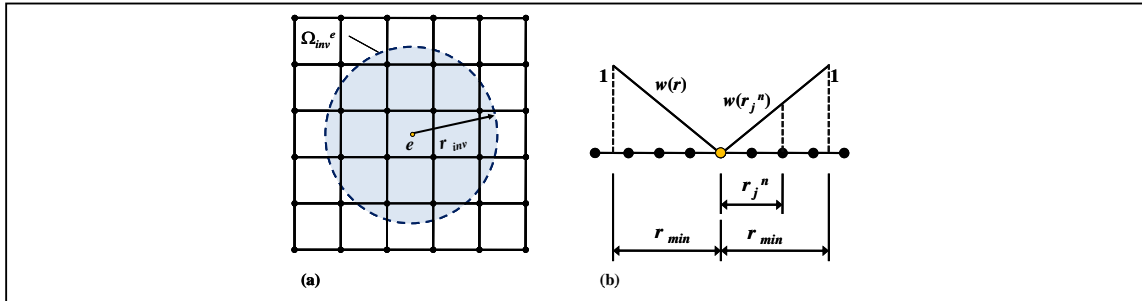


Figure 2: Inverse projection scheme: (a) domain Ω_{inv}^e ; (b) linear weight function

The proposed inverse projection scheme consists essentially of an inverse cone of base $2 r_{inv}$ and unit height centered on the circle of radius r_{inv} (Figure 2b). Moreover,

$$\rho^e = \frac{\sum y_j w_{inv}(\mathbf{x}_j - \mathbf{x}^e)}{\sum w_{inv}(\mathbf{x}_j - \mathbf{x}^e)} \quad (5)$$

$$w_{inv}(\mathbf{x}_j - \mathbf{x}^e) = \begin{cases} \frac{r_j^e}{r_{inv}^e} & \text{if } x_j \in \Omega_{inv}^e \\ 0 & \text{if } x_j \notin \Omega_{inv}^e \end{cases} \quad (6)$$

The nodes in the region Ω_{inv}^e are weighted proportionally to the distance between the node and the center of the element as shown in (6), and the element volume fraction ρ^e of element e is evaluated using the nodal variables y_j as shown in (5). The radius r_{inv} indicates that the minimum allowable length scale for any hole corresponds to $2 r_{inv}$, the basis of the inverse projection cone.

4. The minimum compliance problem

Both the direct and the inverse projection schemes were applied to the minimum compliance problem (7), which can be solved using the optimality criteria:

$$\begin{aligned} \min \quad & C(\mathbf{y}) = \mathbf{U}^T \mathbf{K} \mathbf{U} \\ \text{s.t.} \quad & V(\mathbf{y}) = \sum y_j \leq f V_0 \\ & y_{min} \leq y_j \leq 1 \end{aligned} \quad (7)$$

One important feature about the implementation is the procedure to identify the nodes that influence the volume fraction of element e in the direct and in the inverse schemes. Search procedures are expensive, especially for fine meshes and large values of either r_{min} or r_{inv} . As the set of nodes lying in the regions Ω_w^e and Ω_{inv}^e are the same for all the steps of the optimization process, these search procedures are performed only once at the beginning of the algorithm.

5. Results

This section presents a numerical result for both the direct and the inverse schemes for a cantilever beam (Figure 3). The extended domain Ω is fixed along the left edge and has the aspect ratio of 2/1 and unit width. A point load $P = -1$ is applied to the lower left free corner of the beam. The length scale of the direct projection scheme is $d_{min} = 2 r_{min}$ (Figure 1b) and the length scale of the inverse projection scheme is $d_{inv} = 2 r_{inv}$ (Figure 2b). For the sake of simplicity of notation, the length scale of either projection is referred as d .

The problem is solved using 4-node quadrilateral elements and the prescribed volume of the structure is 50% of the domain volume Ω . Continuation technique is applied to the penalization factor of the SIMP model, p , which varies from 1.0 to 3.0 stepping 0.5. The Poisson's ratio is $\nu = 0.25$ and the Young's modulus $E = 10^6$. Consistent units are employed.

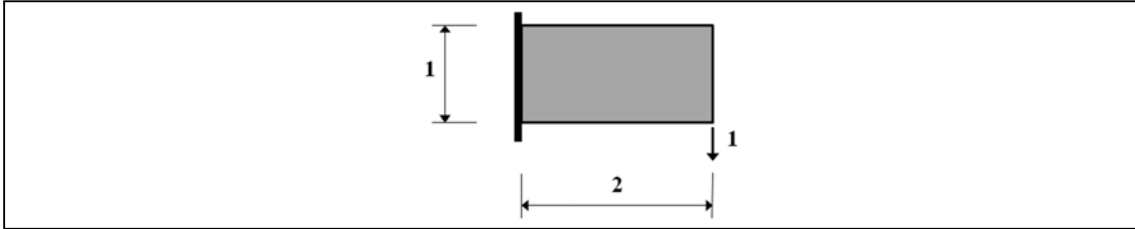


Figure 3: Cantilever beam

Figure 4 shows the results obtained with the direct and the inverse schemes using a mesh of 100 x 50 elements and considering the radius of the projection to be 1 and 2 units. A comparison of Figures 4c and 4d illustrates

the tendency of the inverse projection to join the holes. The white bar represents $2 r_{min}$ in Figures 4a and 4b or $2 r_{inv}$ in Figures 4c and 4d.

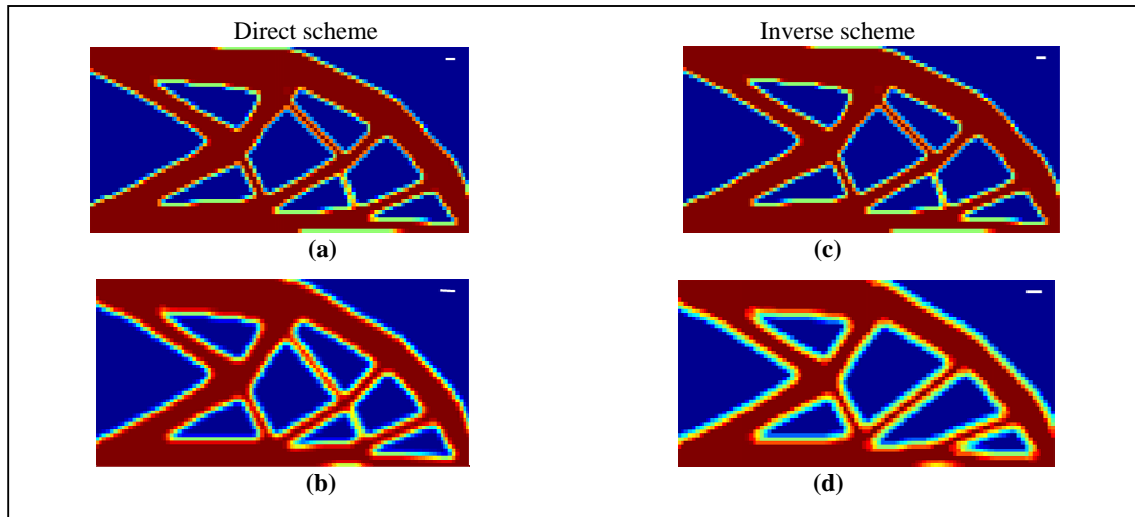


Figure 4: The cantilever beam with mesh 100×50 : (a) $r_{min} = 1$ element; (b) $r_{min} = 2$ elements; (c) $r_{inv} = 1$ element; (d) $r_{inv} = 2$ elements.

6. Conclusions

The inverse projection scheme developed in this paper permits control of the size of holes in topology optimization problems through a mesh-independent process. This work offers room for further extensions. For instance, the inverse projection scheme may be explored with nonlinear projections, which would reduce the intermediate densities obtained with the linear projection. In addition, the present schemes (direct and inverse) can be applied to 3D problems so as combine them to other manufacturing constraints such as symmetry, extrusion and machining. Finally, an improved and robust strategy to combine the direct and the inverse schemes is needed.

Acknowledgement

SRMA acknowledges the Brazilian agency CAPES for financial support. ECNS thanks the Brazilian agencies FAPESP and CNPq and the University of Illinois at Urbana-Champaign (UIUC) for inviting him as a Visiting Professor during the Summer/2007. We gratefully acknowledge the USA NSF through the project CMS#0303492 (Inter-Americas Collaboration in Materials Research and Education, PI Prof. W. Soboyejo, Princeton University).

References

- [1] Bourdin B. Filters in topology optimization. *International Journal for Numerical Methods in Engineering* 2001, **50**:9, 2143-2158.
- [2] Carbonari RC, Silva ECN and Paulino GH. Topology optimization design of functionally graded bimorph-type piezoelectric actuators. *Smart Materials and Structures* 2007, **16**:6, 2605-2620.
- [3] Guest JK, Prévost JH and Belytschko T. Achieving minimum length scale in topology optimization using nodal design variables and projection functions. *International Journal for Numerical Methods in Engineering*, 2004, **61**:2, 238-254.
- [4] Sigmund O. On the design of compliant mechanisms using topology optimization. *Mechanics of Structures and Machines* 1997, **25**:4, 493-524.
- [5] Sigmund O. Design of multiphysics actuators using topology optimization - Part II: Two-material structures. *Computer Methods in Applied Mechanics and Engineering* 2001, **190**:49-50, 6605-6627.

Design of dynamic laminate piezoelectric sensors and actuators using topology optimization

Paulo Henrique NAKASONE*, Emílio Carlos Nelli SILVA

*Polytechnic School of the University of Sao Paulo
Department of Mechatronic and Mechanical Systems Engineering
Av. Prof. Mello de Moraes, 2231 – Butantã – São Paulo – SP – Brasil
paulo.nakasone@poli.usp.br

Abstract

Plate-shaped piezoelectric sensors and actuators have been increasingly used in the field of smart structures. Some of its applications are vibration control of structures, air fan applications, fluid pumping devices and also energy harvesting transducers. This project aims at the development of a finite element and topology optimization software to design laminate piezoelectric sensors and actuators. The design of a piezoelectric transducer using topology optimization consists in distributing piezoelectric material over a metallic plate in order to achieve a desired dynamic behavior with specified vibration frequencies. The piezoelectric finite element applied is based on the MITC formulation, which is reliable, efficient and avoids the shear locking problem. The bonding between and metallic plates is based on the layer-wise model. The topology optimization formulation is based on the PEMAP-P model (Piezoelectric Material with Penalization and Polarization) and RAMP (Rational Approximation of Material Properties), where the design variables are pseudo-densities that describe the amount of material and polarity of the piezoelectric at each finite element. A multi-objective function is defined in this optimization problem. At the same time the mean transduction is maximized to achieve higher conversion of electric energy into elastic energy, the mean-compliance is minimized to prevent the structure of becoming excessively flexible, and the eigenvalues are optimized to tune the structure for a given frequency. This paper presents the implementation of the finite element and optimization software and shows preliminary results achieved.

1. Introduction

Laminate piezoelectric devices have been widely applied as smart structures, for sensing, actuating and also energy harvesting applications. Most recently, piezoelectric laminates have found applications in the fluidics area, such as air fan (Açikalin *et al.* [1]) or fluid pumping devices (Vatanabe *et al.* [2]) applied to cooling systems designed to handle the increase of power and heat generation in electronic equipments.

Piezoelectric laminates have been studied through analytical and numerical methods (DeVoe and Pisano [3], Fernandes and Pouget [4]). The distribution of piezoelectric material within material layers affects the performance, hence, distribution, amount, shape, size and placement of material should be simultaneously considered in a design optimization problem. Some authors started applying optimization algorithms to distribute piezoelectric material (see Frecker [5] for more details) through parametric optimization, which requires a previous knowledge of shape and number of actuators to be placed. Most recently, more advanced techniques, such as topology optimization have been applied to the design of piezoelectric laminates for static loads (Kögl and Silva [6]). The use of topology optimization techniques allows a free distribution of material over a design domain without constraints related to location, number or shape of transducers.

The present work aims at applying the Topology Optimization Method to the design of laminate piezoelectric devices by distributing piezoelectric material over an elastic base layer in order to achieve maximum displacements at certain points of the structure, taking into account the dynamic response of the system, which is a novel approach to design piezoelectric laminate devices.

Designing sensors and actuators using Topology Optimization demands two different approaches, meaning that two different objective functions are formulated to distribute piezoelectric material over a design domain (Γ_u). In the case of an actuator, we must maximize the output displacement (u^{max}) considering a given input charge applied (\bar{Q}), as shown in Figure 1(a) above. However, to design a sensor, it is desired to maximize the output voltage (φ^{max}) for a given force or set of forces (F_A), as shown in Figure 2(b).

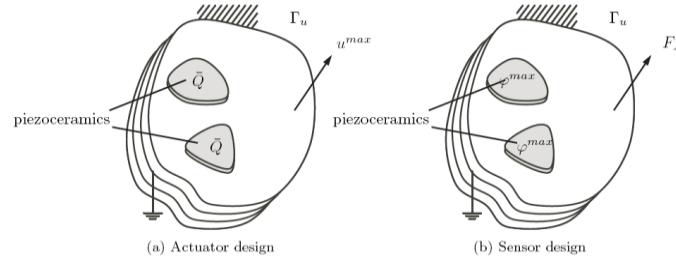


Figure 1: Design of piezoelectric sensors and actuators

2. Piezoelectric Finite Element Plate

In this work, a Reissner-Mindlin plate model is used to model the plate. To avoid the shear-locking problem, the MITC approach is used within the element proposed by Kögl and Bucalem [7]. The element has five mechanical and one electrical degree of freedom at each node and also an element degree of freedom that represents the electrode voltage. The electrical degree of freedom at each node allows a representation of both applied electric potential and the potential induced by elastic deformation. To model the perfect bonding between plates, a layer-wise model is used.

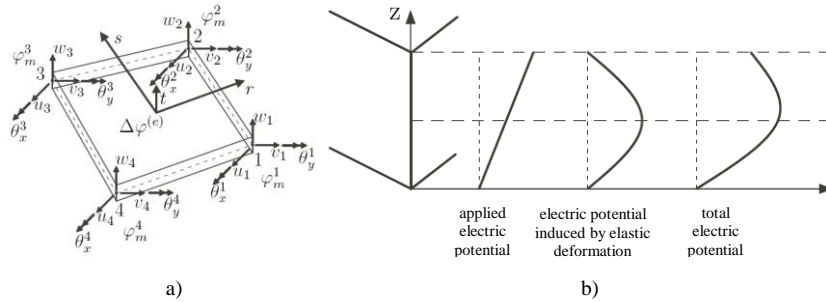


Figure 2: (a) Piezoelectric plate element; (b) Electric potential in thickness direction

3. Topology Optimization Method

The work applies the Topology Optimization Method, which is a powerful structural optimization technique that combines the Finite Element Method with an optimization algorithm to set an optimal material distribution inside a given design domain. The main issue to be addressed in the topology optimization is how to change the material density ρ_l between 0 (void) and 1 (solid material). The use of discrete values is ill-posed due to the multiple local minima and should therefore, be avoided. The problem can be relaxed during the optimization by allowing it to assume intermediate densities, which is achieved by setting an appropriate continuous material model.

This work employs the PEMP-P model combined with the RAMP model, which minimizes the grayscale appearance in topology optimization problems, leading to the following material model:

$$\begin{aligned} \mathbf{C} &= \mathbf{C}_{\min} + \frac{\rho_l}{1 + p_c(1 - \rho_l)} (\mathbf{C}_0 - \mathbf{C}_{\min}) \\ \mathbf{e} &= \rho_l^{p_c} (2\rho_l - 1)^{p_c} \mathbf{e}_0 \\ \boldsymbol{\varepsilon} &= \rho_l^{p_c} \boldsymbol{\varepsilon}_0 \end{aligned} \quad (1)$$

where: \mathbf{C}_0 , \mathbf{e}_0 and $\boldsymbol{\varepsilon}_0$ are the elasticity, piezoelectricity and permittivity matrices of the material and \mathbf{C}_{\min} is a minimum value for the elasticity \mathbf{C} . The ρ_2 variable defines the material polarization, where $\rho_2 = 1$ when the polarization is positive and $\rho_2 = 0$ when the polarization is negative.

4. Design Problem Formulation

To achieve the goals proposed in this work, it is necessary to combine different design formulation problems in a multi-objective function: maximization of mean transduction; minimization of mean compliance; and optimization of the mean-eigenvalue.

4.1 Maximization of Mean Transduction

The mean transduction describes the conversion of electrical into elastic energy and vice-versa using two different electro-elastic states resulting from two different load cases that are applied to the structure. By properly choosing these load cases, L_{21} becomes proportional to the displacement u^{max} or the output potential ϕ^{max} . The mean transduction is calculated by:

$$L_{21} = \hat{\mathbf{U}}_2^T \hat{\mathbf{Q}}_1 = \hat{\mathbf{U}}_2^T \mathbf{K} \hat{\mathbf{U}}_1 \quad (2)$$

4.2 Minimization of Mean Compliance

To avoid the optimization algorithm to find an overly flexible structure, the mean compliance of the structure can be maximized. This problem is not so relevant when a base-layer remains fixed during the optimization, but it can be necessary if all layers take part into the optimization procedure. The mean compliance is given by:

$$L_{33} = \hat{\mathbf{U}}_3^T \hat{\mathbf{Q}}_3 = \hat{\mathbf{U}}_3^T \mathbf{K} \hat{\mathbf{U}}_3 \quad (3)$$

4.3 Optimization of the mean eigenvalue

To design piezoelectric transducers considering its dynamic behavior, it is necessary to introduce the mean-eigenvalue concept (for more details see Ma *et al.* [7])

$$\Lambda = \left[\alpha \sum_{i=1}^m w_i (\lambda_i - \lambda_{ei})^2 \right]^{1/2} \quad (4)$$

where: α and w_i are weighting coefficients, λ_i is the i^{th} eigenvalue of a structure, λ_{ei} is the i^{th} desired eigenvalue and m is the number of eigenvalues considered in the optimization problem. Thus, minimizing Λ means minimizing the difference between the structure stiffness and the desired eigenfrequencies. Once this work seems not to be strongly affected by switching modes, we can set $m=1$ and design only the first eigenvalue. The weighting coefficients can be set to unity and the square root can be eliminated. Additionally, to combine the three design problems into one multi-objective function, it is interesting to have the logarithm values analyzed, in order to normalize the quantities taken into account in the optimization problem, leading to:

$$\Lambda = [\ln(\lambda_e) - \ln(\lambda)]^2 \quad (5)$$

4.4 Formulation of the Multi-Objective Function

In this work, additionally to the optimization problems addressed by Kögl and Silva [6], it considers the mean eigenvalue problem, that aims at tuning the structure for a desired eigenvalue. The optimization problem is formulated as:

$$\begin{array}{l} \text{minimize } F = (1 - w_f) [w_s \ln(L_{21}) - (1 - w_s) \ln(L_{33})] - w_f [\ln(\lambda_e) - \ln(\lambda)]^2 \\ \rho_1, \rho_2 \\ \text{such that: } \mathbf{K} \hat{\mathbf{U}} = \hat{\mathbf{F}}; 0 \leq \rho_{\min} \leq \rho_1 \leq 1; 0 \leq \rho_2 \leq 1; \Theta_0 \leq \Theta(\rho_1) \leq \Theta_1 \end{array} \quad (6)$$

where: FEM equilibrium equations are satisfied, ρ_1 and ρ_2 variables and the volume fraction, $\Theta(\rho_1)$, of distributed material lies within defined boundaries. The optimization problem is solved by using SLP (sequential linear programming)

5. Result

The following result considers a square domain clamped in two opposite sides (L_1 and L_2), and a unitary force is applied at the point A. The optimization process looks for a transducer that maximizes the output voltage of the laminate and also tunes the structure to a desired eigenvalue.

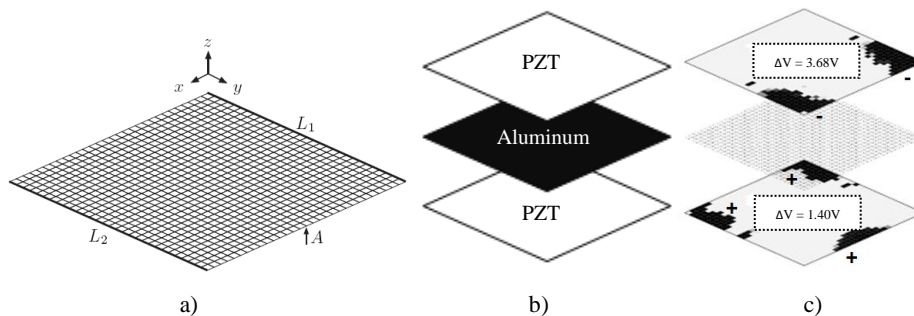


Figure 3: (a) FE mesh; (b) Material layers; (c) Optimization design result

Figure 3(a) shows the mesh used in the optimization. The design domain is $0.3 \times 0.3m$ and has 30×30 elements. The target frequency is set to 60Hz. The base layer is made of aluminum and upper and lower layers are made of PZT as shown in Figure 3(b). The achieved result is shown in Figure 3(c). The output voltage is 3.68V and 1.04V in the upper and lower layers, respectively. The resonance frequency of this device is 57.14Hz.

6. Conclusion

The approach used in this work is robust to design piezoelectric laminated transducers with a specified eigenvalue. The resonance frequency has shown a 5% deviation of the target frequency. The use of the RAMP material model improved the quality of the results, minimizing the grayscale appearance.

7. Acknowledgement

The authors would like to acknowledge FAPESP for the scholarship provided to this project (grant number: 2006/50640-2).

References

- [1] Açikalin T, Wait SM, Garimella SV, Raman A. Experimental investigation of the thermal performance of piezoelectric fans. *Heat Transfer Engineering* 2004; **25**:4-14.
- [2] Vatanabe SL, Pires RF, Nakasone PH, Silva ECN. New configurations of oscillatory flow pumps using bimorph piezoelectric actuators. In *SPIE Smart Structures and Materials & Nondestructive Evaluation and Health Monitoring*, 2008.
- [3] DeVoe DL, Pisano AP. Modelling and optimal design of piezoelectric cantilever microactuators. *Journal of Microelectromechanical Systems* 1997; **6**: 266-270.
- [4] Fernandes A, Pouget J. Analytical and numerical approaches to piezoelectric bimorph. *International Journal of Solids and Structures* 2003; **40**:4331-4352
- [5] Frecker MI. Recent advances in optimization of smart structures and actuators. *Journal of Intelligent Material Systems and Structures* 2003; **14**:207-216.
- [6] Kögl M, Silva ECN. Topology optimization of smart structures: design of piezoelectric plate and shell actuators. *Smart Materials and Structures* 2005; **14**:387-399.
- [7] Kögl M, Bucalem ML. Analysis of smart laminates using piezoelectric MITC plate and shell elements. *Computers and Structures* 2005. **83**: 1153-1163.
- [8] Ma ZD, Kikuchi N, Cheng HC. Topological design for vibrating structures. *Computer methods in applied mechanics and Engineering* 1995. **121**:259-280.